SRESA's International Journal of

LIFE CYCLE RELIABILITY AND SAFETY ENGINEERING

Vol.5 Issue No.1 Jan–March 2016 ISSN – 2250 0820

SOCIETY FOR RELIABILITY AND SAFETY

Typeset & Printed

EBENEZER PRINTING HOUSE
Unit No. 5 & 11, 2nd Floor, Hind Services Industries,
Veer Savarkar Marg,
Dadar (west), Mumbai -28
Tel.: 2446 2632/ 3872
E-mail: outwork@gmail.com

Life Cycle Reliability and Safety Engineering
Vol.5 Issue 1 (2016) 01-07

Convex Modeling of Uncertainties for Service Life Design of RC Bridge Girders Exposed to Marine Environment

Ahsana P.V.[1], K. Balaji Rao[2], M.B. Anoop[2]
[1]*Academy of Scientific and Innovative Research,*
[2]*CSIR-Structural Engineering Research Centre, CSIR Campus, Taramani, Chennai 600113, India*
Email: balaji@serc.res.in

Abstract

The need for probability-based service life design of reinforced concrete (RC) structures subjected to chloride-induced corrosion of reinforcement is well brought out in the literature. However, in most cases sufficient information about the basic variables may not be available to characterize as random variables. In such cases, concepts of convex sets can be used to model uncertainties in engineering problems, as illustrated in this paper. The process of chloride induced corrosion and uncertainties associated with the variables describing the phenomenon, are dealt with in two stages: initiation and propagation. Uncertainties in the variables influencing these stages of corrosion process are modeled by ellipsoid bound uncertainty model,embedding a desired level of robustness. A methodology is developed for service life design, involving two optimization routines, one in each stage of corrosion, and taking the uncertainties into account through convex models. The ultimate aim is to find the initial diameter of the tensile reinforcement to be provided, satisfying multiple performance criteria at desired ages of the girder. A designer has different options to enhance durability of the girder, i.e.through better quality of workmanship, higher grade of concrete, larger clear cover to the reinforcement etc. However, this paper considers only the increase in tension bar diameter as the option to ensure desired performance during the service life. A failure analysis of Rocky Point viaduct is carried out for illustration, and the initial diameter of tensile bar that should have been provided to meet pre-fixed performance criteria during the service life is determined. The paper brings out the potential of this non-stochastic approach of handling uncertainties in engineering applications.

Keywords: *Convex modelling, service life design, RC bridge, marine environment*

1. Introduction

All engineering structures experience degradation of strength with time due to environmental effects in addition to the other loads they are subjected to during their service life. Among many of the potential degradation mechanisms ofreinforced concrete structures, chloride induced corrosion of the reinforcing steel is identified as one of the major causes of premature repair/rehabilitation. The process of chloride induced corrosion and its influence on behaviour of reinforced concrete structures are beset with uncertainties and hence, it is important to handle them in decision making. This problem has been thoroughly researched by experimental and analytical methods during past few decades, a few of the important contributions are mentioned below.

Pioneers like Tuutti[1] gave the basic corrosion initiation and propagation models. Later, the mechanism of corrosion in RC members, starting from the initiation of corrosion (Collerpardi et al[2], Enright and Frangopol[3], Kirkpatrick et al[4]), to the propagation leading to cracking/spalling of cover concrete (Liu and Weyers[5], Alonso et al[6], Xia and Jin[7]) is very well investigated over the years. Corrosion in marine environments was elaborately studied by Melchers and Li[8]. Statistical model for concentration of chloride in concrete was proposed by Engelund and Sorensen[9]. Improvements to existing corrosion deterioration models and life-cycle reliability models were proposed by Vu and Stewart[10]. Enright and Frangopol[3,11] published statistical characteristics of material properties and analytical degradation models based on investigations on existing structures. Most recent works of Possan and Andrade[12] involve probabilistic modelling of degradation of concrete members by using homogeneous Markov chains.

Probability based methodologies have been the most popular tools for handling uncertainties in the process of corrosion and in characterising its influence on structural behaviour. But, many times, sufficient data may not be available to assign probability distributions to some of the uncertain variables associated the corrosion process. In such case, convex set modeling (Ben-haim[13]) can be used as an alternative method to probabilistic modeling.

Corrosion initiation in RC members, viewed through thermodynamics point of view, is a process exhibiting bifurcation and hence is expected to show large variations (Pande *et al*.[14]). In such situations, to establish the robustness of the design, it is preferable to model the variations in T_i by a convex set. The convexity theorem, just as central limit theorem in the case of probability theory, will help in modeling the T_i as a convex set. When the response of a system is modeled as a convex set, determination of reliability or robustness of the system would involve determination of maximum variations in basic variables that the system can withstand by ensuring that the responses are within the specified limits. In this paper, an attempt is made to determine the minimum value of a basic design variable to keep $(T_i)_{\min}$ > service life of structure. One of the advantages of using convex sets is that the optimization problems can be handled efficiently.

The process of chloride induced corrosion and uncertainties associated are dealt in two stages: initiation and propagation. Initiation is assumed to be due to accumulation of sufficient amount of chlorides near the reinforcing bars, which are diffused from the external environment to inside of concrete due to a concentration gradient. Fick's second law of diffusion is assumed to be valid. The second phase, propagation of corrosion is dependent on corrosion rate, which in turn is dependent on the corrosion current density and pitting factor. In this paper, important variables involved in describing the aforementioned two stages are modeled as convex sets. Modeling of uncertainties using convex set concept is discussed below.

2. Uncertainty Handling in the Corrosion Intiation Stage

The ingress of chlorides through the cover concrete of an RC member loaded in marine environment is, generally, governed by Fick's second law of diffusion. Accordingly, the corrosion initiation time, T_i, is given by

$$T_i = \frac{\tilde{c}^2}{4D}\left\{erf^{-1}\left(\frac{c_0 - c_{cr}}{c_0}\right)\right\}^{-2} \quad (1)$$

where $\tilde{c}$, D, c_0 and c_{cr} are respectively clear cover to reinforcement, diffusion coefficient, surface chloride content and critical chloride content. While $\tilde{c}$ and D can be considered to depend on quality of workmanship, c_0 depends on exposure conditions and c_{cr} depends on type of concrete and steel. While in most of the investigations, these variables are considered as random, it may be better to model them as convex variables/sets when sufficient information is not available to fit pdf. The variables to be included in the uncertainty analysis can be based on a sensitivity analysis that is presented in the next section.

Sensitivity Analysis on T_i

Relative sensitivity (RS) of the four basic variables affecting T_i is carried out to compare the importance of individual variable. In general, relative sensitivity (RS) of individual variable (v_i) of a function $F = f(v_1, v_2, \dots, v_n)$ is given by

$$RS(v_i) = \frac{\partial F}{\partial v_i}\frac{v_i}{F}, i = 1, \cdots, n \quad (2)$$

In the case of $T_{i,}$

$$T_i = f(\tilde{c}, D, c_0, c_{cr}) \quad (3)$$

For example, relative sensitivity of the variable clear cover is, $RS(\tilde{c}) = \frac{\partial T_i}{\partial \tilde{c}}\frac{\tilde{c}}{T_i}$ (4)

Values of the relative sensitivity factors are computed at the nominal value (i.e., the mean value) of the uncertain variables. Partial derivatives of the functionT_i are given below.

$$\frac{\partial T_i}{\partial \tilde{c}} = \frac{2\tilde{c}}{4D}\left\{erf^{-1}\left(\frac{c_0 - c_{cr}}{c_0}\right)\right\}^{-2}$$

$$\frac{\partial T_i}{\partial D} = \frac{-\tilde{c}^2}{4D^2}\left\{erf^{-1}\left(\frac{c_0 - c_{cr}}{c_0}\right)\right\}^{-2}$$

$$\frac{\partial T_i}{\partial c_0} = \frac{-\tilde{c}^2\sqrt{\pi}}{4D}\frac{c_{cr}}{c_0^2}\left\{\mathrm{erf}^{-1}\left(\frac{c_0 - c_{cr}}{c_0}\right)\right\}^{-3}\exp\left[-\left\{\mathrm{erf}^{-1}\left(\frac{c_0 - c_{cr}}{c_0}\right)\right\}^2\right]$$

$$\frac{\partial T_i}{\partial c_{cr}} = \frac{-\tilde{c}^2\sqrt{\pi}}{4D}\left\{\mathrm{erf}^{-1}\left(\frac{c_0 - c_{cr}}{c_0}\right)\right\}^{-3}\exp\left[-\left\{\mathrm{erf}^{-1}\left(\frac{c_0 - c_{cr}}{c_0}\right)\right\}^2\right] \quad (5)$$

In order to select the most sensitive variables affecting corrosion initiation, relative sensitivity analysis is carried out for two types of concrete, viz. OPC and 30% PFA concretes. Nominal values of the four variables are taken as 5cm, 4.89sqcm/year, 0.3 % weight of concrete and 0.125 % weight of concrete for OPC concrete girder, and 5cm, 0.20sqcm/year, 0.5 % weight of concrete and 0.1% weight of concrete

for 30%PFA concrete girder, respectively (Enright and Frangopol[3], Bamforth[15] and Balaji Rao and Anoop[16]).Results of the relative sensitivity analysis is presented in Table (1). From the absolute values of RS, it is noted that T_i is most sensitive to C , D and c_0 for both the types of concrete. Hence, uncertainties in these variables need to be considered in characterizing the uncertainties associated with T_i. In this paper, these variables are modeled as convex variables. It is assumed that the values of these variables can vary with respect to their nominal values. As pointed out in Ben-Haim[13], the joint uncertainties in the three significant convex variables can be represented in the form of ellipsoidal bound model. The orientation of the ellipsoid is a measure of the relative sensitivity while the size of the ellipsoid gives a measure of degree of uncertainty. The size of the ellipsoid, β, can be taken as a measure of the robustness of the design when the problem is posed as an analysis problem. In the following section, the formulation of ellipsoid bound model with respect to T_i is presented.

Table 1: Results of relative sensitivity analysis of T_i

	$\tilde{c}$,	D	c_0	c_{cr}
OPC	2	-1	-0.9246	0.2724
PFA	2	-1	-0.1721	0.086

3. Formulation of Ellipsoid Bound Model of Uncertainty

The ellipsoid of uncertainty of a number of variables can be represented by

$$u^T W u \leq \beta^2 \tag{6}$$

Where W is the positive definite matrix of the correlation between the variables, u is the vector of normalized uncertain variables, in this case given by

$$u = \left[\frac{\tilde{c}-\bar{\tilde{c}}}{\bar{\tilde{c}}} \ , \ \frac{D-\bar{D}}{\bar{D}} \ , \ \frac{c_0-\overline{c_0}}{\overline{c_0}}\right]^T \tag{7}$$

where $\bar{\tilde{c}}$, $\bar{D}$ and $\overline{c_0}$ are the mean values of these variables, and β is the required robust reliability with respect to the uncertainties in $\bar{\tilde{c}}$, $\bar{D}$ and $\overline{c_0}$.

Since $\bar{\tilde{c}}$, $\bar{D}$ and $\overline{c_0}$ are independent quantities, W will be a identity matrix of order 3.

$$W = \begin{bmatrix} 1 & 0 & 0 \\ 0 & 1 & 0 \\ 0 & 0 & 1 \end{bmatrix} \tag{8}$$

Substituting Equations (7) and (8) in (6), gives the ellipsoid bound as

$$\left(\frac{\tilde{c}-\bar{\tilde{c}}}{\bar{\tilde{c}}}\right)^2 + \left(\frac{D-\bar{D}}{\bar{D}}\right)^2 + \left(\frac{c_0-\overline{c_0}}{\overline{c_0}}\right)^2 \leq \beta^2 \tag{9}$$

Taking the extreme of the convex set, and normalizing with the robust reliability, β, we get,

$$\frac{\left(\tilde{c}-\bar{\tilde{c}}\right)^2}{\left(\beta\bar{\tilde{c}}\right)^2} + \frac{\left(D-\bar{D}\right)^2}{\left(\beta\bar{D}\right)^2} + \frac{\left(c_0-\overline{c_0}\right)^2}{\left(\beta\overline{c_0}\right)^2} = 1 \tag{10}$$

The problem of evaluation of initiation time, which is a robust reliability analysis problem, under the given uncertainties in basic variables, forms an optimization problem with three unknown variables, with a convex set (ellipsoid) as a nonlinear constraint (Equation (9)). In addition, there are other constraints which make the problem physically meaningful and feasible, like the fact that surface chloride concentration should be greater than the critical chloride concentration for corrosion process to even begin. A minimization routine using genetic algorithm and subsequent gradient based algorithm gives the minimum T_i possible, under these constraints. Similarly, a maximization routine gives the maximum possible T_i under these constraints. Thus, for the given convex set of basic variables, the bounds on T_i can be determined.

4. Uncertainty Handling in the Corrosion Propagation Stage

Propagation of corrosion after the initiation, is governed by corrosion current density (i_{corr}) and pitting factor (α). Uncertainty in the propagation stage is modelled by a convex ellipsoid model of i_{corr} and a. Minimum initiation time obtained from the initiation stage is used in the propagation stage. Objective of modeling uncertainties in the propagation stage is to evaluate the area of tensile steel to be provided under these uncertainties, to meet the required performance criteria at different timesduringthe service life of the structure (an RC girder in this paper). As mentioned in the initiation stage, this problem is also an optimization problem with convex constraints, maximization of which gives the tensile steel area to be provided. (The preliminary cross-sectional dimensions can be obtained from the design according to the code). In contrast to the initiation problem, this may be viewed as a robust design problem since the optimal area of steel is obtained satisfying the performance requirements at different times of service life of the structure.

Ellipsoid bound model which forms the constraint of the optimization is given by:

$$u'^{T} W' u' \le \gamma^2 \quad (11)$$

where γ is the robust reliability required in the system, u' is the vector of convexvariables, given by Equation (12) and W' is the positive definite matrix of order 2.

$$u' = \begin{bmatrix} \frac{i_{corr} - \overline{i_{corr}}}{\overline{i_{corr}}} & \frac{\alpha - \overline{\alpha}}{\overline{\alpha}} \end{bmatrix}^T \quad (12)$$

$$\text{and } W' = \begin{bmatrix} 1 & 0 \\ 0 & 1 \end{bmatrix} \quad (13)$$

Substituting Equations (12) and (13) in Equation (11) and considering the equality constraint, equation of ellipse is obtained as,

$$\frac{\left(i_{corr} - \overline{i_{corr}}\right)^2}{\left(\gamma \overline{i_{corr}}\right)^2} + \frac{\left(\alpha - \overline{\alpha}\right)^2}{\left(\gamma \overline{\alpha}\right)^2} = 1 \quad (14)$$

This will form the convex constraint to the optimization for initial diameter of reinforcing bar to be provided, in order to satisfy required performance criteria. In the present paper, the performance criteria are based on percentage loss of capacity at different times during the service life of the structure. The percentages considered are 5%, 10% and 25%. It may be noted that this criteria may not be met with for some of the design scenarios as the original area of the steel to be provided may exceed the maximum allowable values according to code.

5. Robust Design Procedure

Step 1: Design the girder according to a code of practice. (Fix clear cover and other concrete section dimensions. Obtain the area of tension steel required to resist the specified nominal loads.)

Step 2: Evaluate bounds of corrosion initiation time T_i for the designed section, under the uncertainties defined by robust reliability β, through constrained optimization.

Objective function: $T_i - \frac{\tilde{c}^2}{4D}\left\{erf^{-1}\left(\frac{c_0 - c_{cr}}{c_0}\right)\right\}^{-2} = 0$ (15)

Constraints: Equation (10)

Bounds of the uncertain variables $\tilde{c}$, D and $c_{0,}$ will depend on the values of mean of the corresponding variable and robust reliability factor, β, in the constraint equation. Lower and upper bounds of a variable are given by *mean value*×*(1±β)*.

Step 3: Define instances of time, at which certain performance criteria are reached. Example: T_5- time at which at least 95% of initial flexural capacity is available, T_{10}- time at which at least 90% of initial flexural capacity is available, T_{25}- time at which at least 75% of initial flexural capacity is available etc. For the service life design, the designer can also specify the time (age) at which these performance criteria can be acceptable.

Step 4: Evaluate the reduced area of tensile steel $A_{st}(t)$, corresponding to the flexural capacities as stipulated, at the corresponding time instances- T_5, T_{10} and T_{25}.

Step 5: Decide the robust reliability, γ in the convex variables i_{corr} and α .

Step 6: Evaluate the bounds of initial area of steel A_0 to be provided to satisfy all the performance criteria stipulated, through constraint optimization. The value of T_i is taken as the minimum T_i obtained by optimization in Step 2, for obtaining conservative results.

In order to estimate the capacities at different times, into the propagation phase, the remaining area of steel is required. The same is computed from

$$A_{st}(t) = \frac{n_1\pi}{4}\phi(0)^2 + \frac{n_2\pi}{4}\phi(t)^2 = \frac{n_1\pi}{4}\phi(0)^2 + \frac{n_2\pi}{4}[\phi(0) - 0.0115 i_{corr}\alpha(t - T_i)]^2 \quad (16)$$

Where n_1 and n_2 are the number of uncorroding and corroding bars; ϕ(0) is the unknown initial diameter of bars and ϕ(*t*) is the remainingdiameter of the corroded bars.

$$\frac{(n_1 + n_2)\pi}{4}\phi(0)^2 - 2\frac{n_2\pi}{4} r_{corr}(t - T_i)\phi(0) + \frac{n_2\pi}{4}[r_{corr}(t - T_i)]^2 - A_{st}(t) = 0 \quad (17)$$

This is a quadratic equation in φ(0). "Keeping the number of bars as the same as obtained from preliminary design", φ(0) is the only unknown in the above equation and can be solved by constrained optimization on uncertain variables i_{corr} and α. Lower and upper bounds of the variables will be fixed by the constraint equation, depending on the mean value of the variable and the value of robust reliability factor as mentioned before.

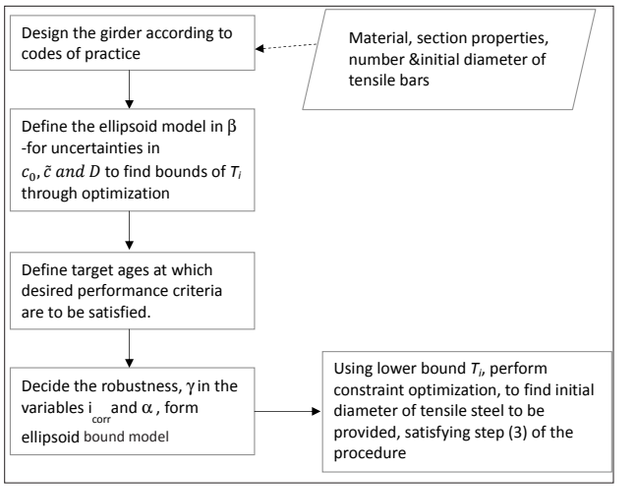

Figure 1 Design flow chart for service life design

Objective function: derived from Equation (17).

Constraint: Equation (14).

A design flowchart of the proposed methodology is presented in Figure (1).

5.1 Example: Rocky Point Viaduct Failure Analysis

The Rocky Point Viaduct, located near Port Orford, Oregon, at a coastal site 25 miles east of Pacific Ocean, is considered for the example (Covino et al, [17], Cramer et al, [18]). The Viaduct had 5 spans with a total length of 114 m and a deck width of 10.6 m. First repair of the viaduct due to excessive corrosion of reinforcement considered in the case-study

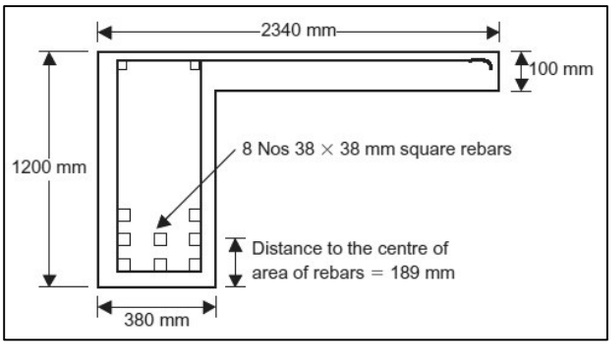

Figure. 2 *Cross-sectional details of the edge beam of Rocky Point Viaduct considered in the case-study*

was carried out within 14 years of construction in 1955. The whole structure was later replaced in 1991. Cross section of one exterior L-beam is shown in Figure (2).

Detailed investigation of the edge beam was performed at laboratories which showed that excessive corrosion of reinforcing bars, on the exterior sides of the girder was the reason to failure (Covino et al [17], Cramer[18]). Chloride concentration at the level of middle bars was still below critical concentration to initiate corrosion. In this study, it is assumed that only the side bars are corroding with time. Equivalent round bars are considered for analysis, instead of square bars. In this example, three performance criteria are considered, T_5, T_{10} and T_{25} as 20, 30 and 50 years respectively. Robust design involves determination of optimal initial diameter of steel (or area of steel) satisfying all the criteria.

Table 2: Details of the Rocky Point Viaduct*

Variable	Unit	Value
yield strength of steel - f_y	MPa	556
compressive strength of concrete - f_{ck}	MPa	34.16
diameter of longitudinal bar - ϕ(0)	mm	42.5
Mean clear cover for side ofthe girder	cm	6.75
n_1- number of uncorroded bars	-	2
n_2 number of corroding bars	-	6
Mean diffusion coefficient D	sqcm/year	0.4
Mean surface chloride concentration	% wt of concrete	0.4
Critical chloride concentration	% wt of concrete	0.02
Mean corrosion current density	μA/sqcm	4
Mean pitting factor	-	4
Robust reliability w.r.t T_i	-	0.6
Robust reliability w.r.t initial area of steel	-	0.65

(Note*-based on testing of girder (Covino et al [17], Cramer et al [18]))

6. RESULTS AND DISCUSSION

The range of T_i obtained with a required robust reliability β=0.6 along with the optimum values of uncertain variables, are presented in Table 3.

Table 3: Range of T_i obtained corresponding to the optimum values of the convex variables, D and c_0

Optimum values of variables	$\tilde{c}$,	D	c_0	Result of T_i
	(cm)	(sq. cm/ year)	(% wt of concrete)	(years)
For Minimization	5.2	0.5994	0.4970	5.3608
For Maximization	8.2	0.1822	0.3473	51.1791

Initial diameter of tensile steel is obtained for a robust reliability = 0.65. Since the mean values of both the convex variables, namely i_{corr} and α, are numerically the same, the constraint equation effectively becomes that of a circle, which is the special case of an ellipse. The values of i_{corr} and α, which minimize and maximize the initial diameter are obtained through constraint optimization and the same are presented in Table 4. It is observed that numerically the values of i_{corr} and αare the same and the pointson the circle, denoted by the minimizing and maximizing set of values of i_{corr} and αlie diagonally opposite to each other. Initiation time of corrosion, $T_{i,}$ is taken as the minimum value obtained from Table 3, i.e. 5.36 years.

Table 4: Initial diameter of steel to be provided with i_{corr} and α as convex variables

Optimum values of variables	T_i	i_{corr}	α	ϕ (0)
	(years)	(μA/ sqcm)	-	(mm)
For Minimization	5.36	2.1559	2.1559	42.0
For Maximization	5.36	5.8441	5.8441	48.9

The design solution is the maximum value of ϕ, which is 48.9 mm, which satisfies all the three performance criteria stipulated at 20, 30 and 50 years of life of the girder. Minimum value of ϕ does not have a practical significance.

The same methodology can be used to design initial area of steel for longer service life, different performance criteria and various target lives at which the performance criteria are to be met. Table (5) shows the initial area of steel to be provided in different service lives and target ages of performance criteria, for the same exposure conditions and concrete properties. Initiation time of corrosion is taken same as 5.36 years, as obtained in the previous analysis. Upper limit of the diameter obtained is presented in the table, for the reasons mentioned earlier.

Table.5: Initial diameter of reinforcement obtained in various cases

Service life	T_5	T_{10}	T_{25}	ϕ(0)	% area of steel
(years)	(years)	(years)	(years)	(mm)	
50	20	30	50	48.9	3.9%
50	10	20	40	46.2	3.5%
100	30	50	80	56.2	5.1%
100	20	40	70	53.9	4.7%

Care should be taken, so that maximum allowable percentage steel is not exceeded, by providing the steel as per the above methodology. IS 456 (2000) suggests 4% as the maximum percentage of tension steel in flexural beams. From Table (5), it can be observed that, for a girder intended to have 50 years of service life, the initial diameter suggested by the method is acceptable. Whereas, for a longer service life, the permissible percentage steel is exceeded, which means, alternate solutions should be sought, to ensure required service life, like increasing the cover, or changing the material composition etc.

7. Conclusion

In this paper, a service life design methodology is developed, which takes care of uncertainties through convex set concepts. This methodology is very useful when sufficient data is not available to characterize uncertainties in variables with probabilistic approach. Uncertainties in the convex variables are represented by ellipsoid bound models corresponding to two stages of corrosion, namely, initiation and propagation. Details of the Rocky Point viaduct which failed due to corrosion is made use to perform a failure analysis. Through the optimization procedures, it is found that,to satisfy multiple performance criteria of residual flexural capacities of 95%, 90% and 75% at 20, 30 and 50 years respectively, the initial diameter of tensile bar should have been 48.9 mm, for the considered robustness of 0.6 and 0.65 corresponding to the two stages of corrosion.

Acknowledgment

This paper is being published with the kind permission of Director, CSIR-SERC.

References

1. Tuutti, K. (1982). "Corrosion of Reinforcement in Concrete", *Swedish Cement and Concrete Research Institute*, 4, Sweden.
2. Collepardi, M., Marcialis, A., and Turriziani, R. (1972). "Penetration of chloride ions into cementpastes and concretes", *Journal of the American Ceramic Society*, 55 (10), 534–535.
3. Enright, M. P., and Frangopol, D. M. (1998). "Probabilistic analysis of resistance degradation of reinforced concrete bridge beams under corrosion",*Engineering Structures*, 20 (11), 960–971.
4. Kirkpatrick, T. J., Weyers, R. E., Anderson, C. M., and Sprinkel, M. M. (2002). "Probabilistic model for chloride induced corrosion service life of bridge decks", *Cement and Concrete Research*, 32 (12), 1943-1960.
5. Liu, Y., and Weyers, R. E. (1998). "Modelling the time-to-corrosion cracking in chloride contaminated reinforced concrete structures", *ACI Materials Journal*, 95 (6), 675-81.
6. Alonso, C., Andrade, C., Rodriguez, J., and Diez, J. M.

(1998). "Factors controlling cracking of concrete affected by reinforcement corrosion", *Materials and Structures*, 31 (7), 435–441.

7. Xia, J., and Jin, W. (2014). "Prediction of corrosion-induced crack width of corroded reinforced concrete structures*", in proc. 4th International Conference on the Durability of Concrete Structures,* Perdue University, USA.
8. Melchers, R. E., and Li, C. Q. (2009). "Reinforcement corrosion and activation time in concrete structures exposed to severe marine environments", *Cement and Concrete Research*, 39(11), 1068-1076.
9. Engelund, S. and Sorensen, J.D. (1998). "A probabilistic model for chloride-ingress and initation of corrosion in reinforced concrete structures", Structural Safety, 20(1), 69-89.
10. Vu, K.A.T. and Stewart, M.G. (2000), "Structural reliability of concrete bridges including improved chloride-induced corrosion models". Structural Safety, 22, 313-333.
11. Enright, M. P., and Frangopol, D. M. (1998). "Service-life prediction of deteriorating concrete bridges", Journal of Structural Engineering, 124(3), 309-317
12. Possan, E. and Andrade J. J. de O. (2014). "Markov Chains and reliability analysis for reinforced concrete structure service life", Materials Research, 17(3), http://dx.doi.org/10.1590/S1516-14392014005000074
13. Ben-Haim, Y. (1996). *Robust reliability in the mechanical sciences*, Springer -Verlag Berlin Heidelberg.
14. Pande,R. Balaji Rao,K. and Anoop, M.B. "Chloride-induced corrosion initiation in RC structures: a thermodynamic view point", manuscript under preparation.
15. Bamforth, P. B. (1999). "The derivation of input data for modeling chloride ingress from eight-year UK coastal exposure trials", Magazine of Concrete Research, 51(2), 87–96.
16. Balaji Rao, K. and Anoop, M. B. (2014). "Stochastic analysis of reinforced concrete beams with corroded reinforcement", Proceedings of the Institution of Civil Engineers Construction Materials, 167 (CM1), 26–35.
17. Covino, B.S., Cramer, S.D., Holcomb, G.R., Bullard, S.J. and Laylor, H.M. (1999). Postmortem of a failed bridge. Concrete International. 21(2):39-45.
18. Cramer, S.D., Covino, B.S., Holcomb, G.R., Bullard, S.J., Russel, J.H., Dahlin, C.M., Summers, C.A., Laylor, H.M. and Soltesz, S.M. (2000). Evaluation of Rocky Point Viaduct Concrete Beam. Report No. FHWA-OR-RD-00-18, Oregon Department of Transportation, Oregon.

Life Cycle Reliability and Safety Engineering
Vol.5 Issue 1 (2016) 08-17

Reliability Based Code Calibration of Fatigue Design Criteria of Nuclear Class-1 Piping

J. Mishra[1], V. Balasubramaniyan[1], P. Chellapandi[2]
[1]*Safety Research Institute, Atomic Energy Regulatory Board, Kalpakkam, India-603102*
[2]*Bharatiya Nabhikiya Vidyut Nigam (BHAVINI) Ltd. Kalpakkam -603102, India*
Email: jmishra@igcar.gov.in

Abstract

Fatigue design of Class-1 piping of NPP is carried out using Section-III of American Society of Mechanical Engineers (ASME) Boiler and Pressure Vessel code. The fatigue design criteria of ASME are based on the concept of safety factor, which does not provide means for the management of uncertainties for consistently reliable and economical designs. In this regards, a work is taken up to estimate the implicit reliability level associated with fatigue design criteria of Class-1 piping specified by ASME Section III, NB-3650. As ASME fatigue curve is not in the form of analytical expression, the reliability level of pipeline fittings and joints is evaluated using the mean fatigue curve developed by Argonne National Laboratory (ANL). The methodology employed for reliability evaluation is FORM, HORSM and MCS. The limit state function for fatigue damage is found to be sensitive to eight parameters, which are systematically modelled as stochastic variables during reliability estimation. In conclusion a number of important aspects related to reliability of various piping product and joints are discussed. A computational example illustrates the developed procedure for a typical pipeline.

Keywords : *ASME, Fatigue, FORM, Implicit Reliability, HORSM, Piping Products and Joints*

1. Introduction

The piping design in the American Society of Mechanical Engineers (ASME) Boiler and Pressure Vessel (BPV) code [1] is based on Working Stress Design (WSD) methodology, which relies on the concept of factor of safety in the development of design formulas [2]. This approach began with first ASME code in 1914, which use a single factor to provide adequate protection against particular failure modes. The factor of safety is typically a conservative factor developed to address the various uncertainties in the analytical methods of design, applied loads, strength of material, fabrication, examination, testing and other factors that might affect the performance of the components.

Typically, separate factors are used for the various mode of failure such as bursting, plastic deformation, plastic failure, buckling, creep, fatigue or any other mode of failure that is considered significant for the specific problem. This single factor approach of Section-III for each failure modes worked very well for many years, as it indirectly addresses the issue of varying probabilities and consequences of loads on components. Increases in the allowable stresses for occasional loads, such as wind and earthquake loads, in comparison to sustained loads such as pressure and dead weight load reflect the different probability of occurrence. The differentiation of requirements in terms of Class-1, Class-2 and Class-3 components are obviously indirectly related in their importance to the potential consequence or severity of failure.

However, the reliability of a component design by this section varies considerably because the safety factors are based on experience, experimental data and professional expertise, and not through rigorous risk analysis [3]. Recently, a number of ASME code committees have been examining reliability- based requirements with main objective to provide means for the management of uncertainties for consistently reliable and more economical designs, which meets the target level of reliability under various types of loading conditions.

To meet the target reliability and consistency in design it will be a worthwhile exercise to first estimate the implicit reliability level associated with various failure criteria given in the ASME code. Since

Fatigue Design Curve (FDC) of the ASME Section-III [4] is recently revised, and the test data from which this curve is derived has lot of scatter, a work is taken up to estimate the implicit reliability level associated with fatigue failure criteria of this code. In this paper a code calibration is performed to estimate the implicit reliability level associated with class-1 nuclear piping.

2. ASME Fatigue Design Criteria

The ASME Code was one of the first Codes and Standards to treat design for fatigue life explicitly and first to include specific Code rules to prevent low-cycle fatigue failure. In 1971, Section-III of ASME BPV included the fatigue based criteria for the evaluation of Class-1, 2 and 3 pipelines of Nuclear Power Plant (NPP). The ASME Code, for Class -1 pipelines, used a fatigue evaluation method that is based on fatigue tests of polished bars along with the concept of "stress indices" and with the adjustment for stresses that exceed 3Sm (conceptually, exceed the shakedown limit) [5]. For each class of components, the various loads are classified into four different service levels that vary from Level-A through Level-D. Service Level-A corresponds to operating condition, and fatigue failure criteria are mainly concerned with this service level.

2.1 Class-1 Fatigue Evaluation Method

The Class-1 piping fatigue evaluation method, without significant thermal gradient across wall and devoid of any gross material discontinuities, involves the calculation of the primary-plus-secondary stress range S_n by the equation:

$$S_n = C_1 \frac{P_0 D_0}{2t} + C_2 \frac{D_0}{2I} M_i \tag{1}$$

and the peak stress range by the equation:

$$S_p = K_1 C_1 \frac{P_0 D_0}{2t} + K_2 C_2 \frac{M_i}{Z} \tag{2}$$

If $S_n > 3S_m$ (conceptually the shakedown limits of $2S_y$, but for austenitic steel at high temperature it can become $2.7S_y$), S_p is divided by 2 to convert from stress range to alternating stress amplitude. If $S_n > 3S_m$ the strain range corresponding to the elastic-based calculation will not represent the true strain range accumulated in the piping components. In this case, there will be accumulation of plastic strain along with the recoverable elastic strain. Section-III (NB-3228.3) gives a simple way to deal with this condition using a simplified elastic-plastic analysis that involves multiplying S_p by factor K_e, where K_e is given by

$$K_e = 1 + \frac{1-n}{n(m-1)}\left(\frac{S_n}{3S_m} - 1\right); \quad for\ 3S_m \le S_n \le 3mS_m \tag{3}$$

$$K_e = \frac{1}{n}; \qquad for\ S_n \ge 3mS_m \tag{4}$$

The values of m and n for austenitic steel (a common piping material for NPP piping) are 1.7 and 0.3 respectively. From the design fatigue curve (Fig. I-9.2 of ASME Section-III appendix) design cycles N is estimated using alternating stress amplitude ($S_p/2$). The design fatigue curve are derived from strain-controlled, zero mean strain, fatigue tests of polished bars, by incorporating a factor of safety of 2 on stress or 20 on cycles, whichever is more conservative. If the anticipated number of cumulative fatigue cycles in operation is less than N, then the piping products (e.g., girth butt weld, elbow) is deemed to be acceptable. If there are more than one stress ranges linear cumulative hypothesis is used for total fatigue damage assessment.

2.2 Fatigue Life of Piping Products and Joints

From above description it is observed that there are three parameters, namely stress indices C_2 and K_2 and K_e-factor that affect the fatigue life of piping products and joints. A parametric study is carried out to highlight the effect of these parameters on fatigue life of piping products and joints. Six types of products like straight pipe, girth and longitudinal butt weld, butt welding tee and elbow, and branch connection are taken for the comparison of fatigue life. The stress indices of these six products are shown in the legend of Fig. 1.

Though primary plus secondary stress (S_n) is an important parameter in design of pipeline as it is linked with its shakedown limit, Fig. 1 is plotted with nominal stress range as ordinate to highlight the effect of stress indices C_2. The nominal stress directly reflects the load carrying capacities of these products. If it is presumed that pressure load is negligible in comparison of moment load then the nominal stress in these products is simply S_n/C_2. As expected, relatively higher numbers of cycles is allowed in the straight seamless pipe and longitudinal butt weld as the product of K_2 and C_2 are lower for these piping products. Whereas, lesser numbers of cycles are allowed in the elbow and the branch connection as product of K_2 and C_2 indices are higher for these components. Therefore it can be concluded that ASME fatigue criteria for Class-I piping ensure higher

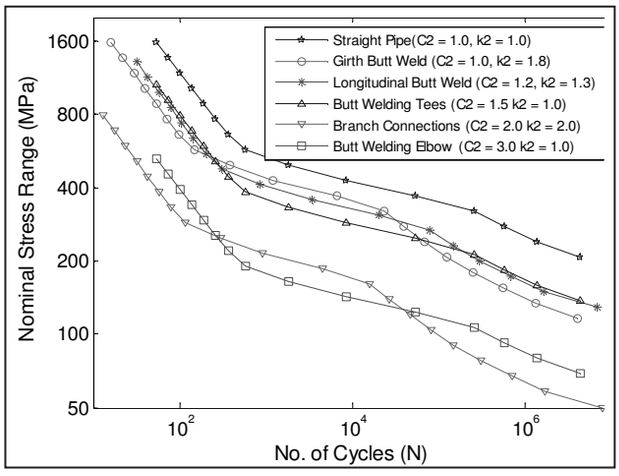

Fig. 1: Allowable number of cycles for piping components w.r.t. nominal stress range (M/Z)

margin for butt welding tees and elbows than girth butt welds and branch connections.

3. Fatigue Curve of ASME and ANL

The ASME Code fatigue design curves, given in Appendix-I of Section-III [4], are based on strain-controlled tests of small polished specimens at room temperature in air. The design curves have been developed from the best-fit curves to the experimental fatigue strain vs. life ($\varepsilon_a - N_f$) data, which are expressed in terms of the Langer equation [6] of the form given in (5):

$$\ln(N_f) = A - B\ln(\varepsilon_a - C) \tag{5}$$

Where ε_a is the applied strain amplitude, N_f is the fatigue life, and A, B and C are coefficients of the model. The ASME Code mean fatigue curves (till 2004 edition) are from the best–fit curves of the experimental data which for austenitic steel is given as:

$$\ln(N_f) = 6.954 - 2.0\ln(\varepsilon_a - 0.167) \tag{6}$$

This fatigue design curves are obtained from the fatigue best-fit curves by first adjusting for the effects of mean stress using the modified Goodman relationship and subsequently reducing the fatigue life at each point on the adjusted best-fit curve by a factor of 2 on strain (or stress) or 20 on cycles, whichever is more conservative. The factors of 2 and 20 are not safety margins but rather adjustment factors that should be applied to the small-specimen data to obtain reasonable estimates of the lives of actual reactor components. Section III criteria document described that these factors were intended to account for data scatter (including material variability) and differences in surface condition and size between the test specimens and actual components.

Recently, Argonne National Laboratory (ANL) after an extensive study of the fatigue database proposed the fatigue best fit curves for austenitic stainless steel [7]. The database consists of large pool of 520 tests carried on smooth specimens under fully reversed strain controlled loading (i.e., R = -1). The database can be segregated into stainless steel type with ≈220 for Type 304 SS; 150 for Type 316 SS; and 150 for Types 316NG, 304L, and 316L SS. The data are shown in the Fig. 2. The proposed fatigue best fit curves for austenitic steel is

$$\ln(N) = 6.891 - 1.920\ln(\varepsilon_a - 0.112) \tag{7}$$

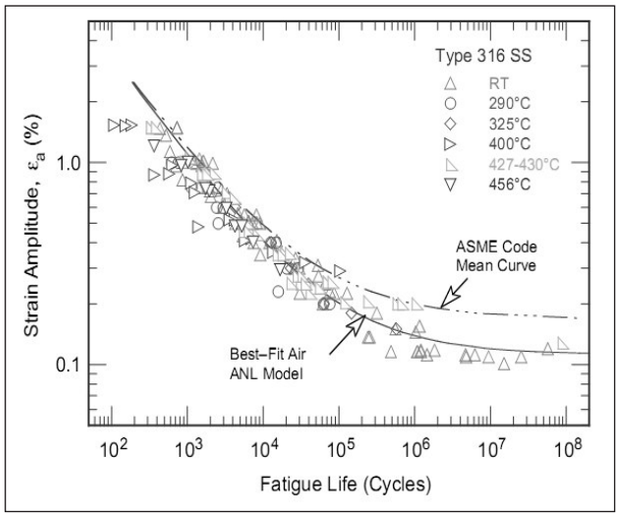

Fig.2: Fatigue ε-N behaviour of 316 Austenitic Stainless Steel in air at various temperatures [7]

The proposed curve is developed by first correcting for mean stress effects, and then reducing the mean–stress adjusted curve by a factor of 2 on stress and 12 on cycles, whichever is more conservative. These factors accounts for the effects of parameters such as mean stress, surface finish, size and geometry, and loading history. A comparison of the ASME (2010) fatigue design curve and ANL fatigue design curve is given in the Fig. 3. The figure shows that the ASME fatigue design curve matches closely with ANL curve. Therefore, for evaluation of implicit reliability associated with fatigue design criteria, limit state formulation is developed based on ANL equation as given in (7).

4. Parameters Affecting Fatigue Life

Fatigue is one of the most frequent causes of failure in the pressure vessels and pipelines. The

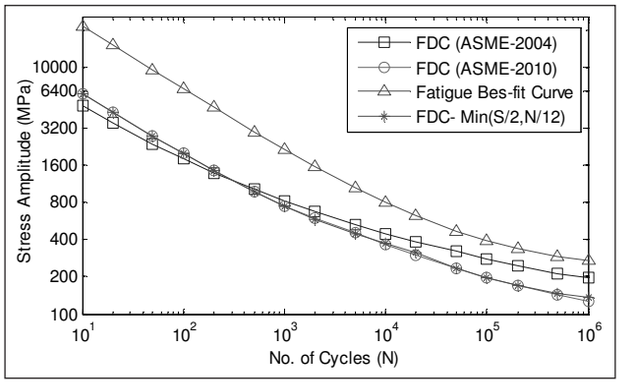

Fig. 3: Fatigue curves for austenitic stainless steel

fatigue life of piping products and joints is sensitive to design details and service conditions such as stress raisers, material properties, welding imperfections, flow induced vibrations, high cycle thermal mixing, thermal stratification, environmental effects etc. [7]. In these components, cyclic loadings occur because of changes in mechanical and thermal loadings as the system goes from one load set (e.g., pressure, temperature, moment, and force loading) to another. The number of cycles applied during the design life of the piping products seldom exceeds 10^5 and is typically less than a few thousand (e.g., low-cycle fatigue).

During cyclic loading of smooth test specimens, surface cracks 10 μm or longer develop early in life (i.e., <10% of life) at surface irregularities. They are either already in existence or produced by slip bands, grain boundaries, second–phase particles etc. Thus, fatigue life may be considered to constitute propagation of cracks from 10 to 3000 μm long [8]. The formation of surface cracks and their growth to an engineering size (3-mm deep) constitute the fatigue life of a material, which is represented by the fatigue ε-N curves. A quantitative description of parameters affecting fatigue life based on data published in the literature is given below:

4.1 Number of Cycle to Failure (N_f)

The number cycle to failure of the components or pipelines is estimated in two steps. In the first step number cycle to failure is estimated in the air environment $N_{air,RT}$. Subsequently a nominal environmental fatigue correction factor $F_{en,nom}$ is used to account the effect of reactor water environment. Then the number cycle to failure can be given as

$$N_f = \frac{N_{air,RT}}{F_{en,nom}} \tag{8}$$

1) Number of Cycle to Failure in Air ($N_{air,RT}$)

The number of cycle to failure in the air environment, $N_{air,RT}$, of a specimen of austenitic stainless steel is obtained from the best fit given by ANL. This equation has three coefficients *A, B* and *C* which are equal to 6.891, 1.920 and 0.112. These coefficients have variability due to data scatter and material variability. The coefficients *B* and *C* have low variability and treated as constants in the probabilistic analysis. Based on the data analysis of 520 tests by ANL, it is observed that the standard deviation of coefficient *A* is 0.417. This leads to the coefficient of variation (COV) of *A* equal to 0.061.

The effects of parameters such as mean stress, surface finish, size and geometry, and loading history, which are known to influence fatigue life, are not explicitly considered in the model given by (7). The Table-I shows the sub-factors on strain (ε) and life (*N*) applied to best-fit fatigue curve for the effects of various parameters in ASME and ANL. The sub-factor given in the [1, 7, 9, 10] are nearly a mean value, whereas range of sub-factor values are given in the ref. [7]. To obtain the stochastic characteristics of the variables, these sub-factors are assumed to follow lognormal distribution with upper and lower limits of

Table 1. Factors on the mean fatigue life to account effects of various parameters

Parameters	Factors on cycles (or Life)				Factor-s on strain
	ASME Section-III	NUREG-CR-			
		6909 [7]	6815 [9]	6717 [10]	6815 & 6717 [9,10]
Material variability and data scatter (min. to mean)	2.0	2.1 - 2.8	2.0	2.5	1.4-1.7
Size effect	2.5	1.2 - 1.4	1.4	1.4	1.25
Surface roughness etc.	4.0	2.0 - 3.5	3.0	2.0-3.0	1.6
Loading histories	--	1.2 - 2.0	1.5-2.5	1.5-2.5	1.3-1.6
Total adjustment	**20**	**6.0 - 27.4**	**12.5-31.0**	10.0-26.0	1.6-1.7

these sub-factors representing the 5th and 95th percentile respectively.

The sub-factor on fatigue life due to Surface Roughness (SR) has the range of value 2.0-3.5. This leads to the mean value and standard deviation of sub-factor on life equal 2.68 and 0.46 respectively. Therefore the COV is equal to 0.17. In the same way, the sub-factor on fatigue life due to Size and Geometry (SG) has the range of value 1.2-1.4. The mean value and standard deviation of this sub-factor on life equal 1.29 and 0.061 respectively. From this, the COV for this sub-factor is equal to 0.046. The load histories are taken care in cumulative damage ratio evaluation.

2) Nominal Environmental Fatigue Correction Factor ($F_{en,nom}$)

The fatigue lives of austenitic SSs are decreased in water environments. The key parameters that influence fatigue life in these environments are temperature, dissolved–oxygen (DO) level in water, strain rate and strain (or stress) amplitude. The environmental effects on fatigue life are significant only when these key parameters meet certain threshold values. When any one of the threshold conditions is not satisfied the environmental effects are moderate, e.g., less than a factor of 2 decrease in life. To quantitatively incorporate the environmental effects in the fatigue design, the number of cycles obtained from fatigue design curve of ASME is adjusted with a nominal environmental fatigue correction factor, $F_{en,nom}$. The $F_{en,nom}$ is defined as the ratio of fatigue life in air at room temperature ($N_{air,RT}$) to that in water at the service temperature (N_{water}) [7,15].

$$F_{en,nom} = \frac{N_{air,RT}}{N_{water}} \tag{9}$$

For wrought and cast austenitic stainless steels it can be given as

$$F_{en,nom} = \exp(0.734 - T'O'\dot{\varepsilon}') \tag{10}$$

Where T' , O' and $\dot{\varepsilon}'$ are transformed temperature, DO level and strain rate respectively defined in [xx]. In the reactor components and pipelines the major fatigue loadings are start-up and planned shutdown of the reactor in its lifetime. These processes occur slowly and the strain rates are very low. Therefore the transformed strain rate ($\dot{\varepsilon}'$) as per [7] will be equal to ($\ln(0.0004/0.4) = 6.91$, which is the maximum value given for strain rate. The operating temperature of light water reactor is in the range of 270-325°C. Also all the thermal cycle will not have temperature going from room temperature to operating temperature. Therefore the transformed temperature (T') is taken as 0.75 corresponding to the operating temperature of 300°C. The transformed DO levels (O') is taken as 0.281.

The nominal environmental fatigue correction factor given by (10) using these values of transformed parameters is 8.93. This value is taken as mean value of the nominal environmental fatigue correction factor. Since, reactor operates at range of temperatures, range of DO levels in coolant as well as range of strain rate, he nominal environmental fatigue correction factor will have large uncertainties in the estimated value. A coefficient of variation equal to 0.15 is taken for further analysis.

4.2. Factor on Strain

The effects material variability, component size, surface finish, and load history on strain do not have cumulative effects of all individual parameters. Rather their effects are controlled by parameter that has the largest effect on life. Therefore, a factor of at least 1.6-1.7 on strain is needed to account for the uncertainties. However, conservatively a factor of 2 on strain is common in design fatigue curve. Since in low cycle fatigue (<10000), factor on cycle is dominant factor. Therefore factor on strain is not considered in this analysis.

5. Formulation For Implicit Reliability Level In Fatigue Design

To evaluate the implicit reliability levels of the code design procedures against a particular failure mode, the first step lies in the definition of a limit state function corresponding to codal provision given for that failure mode. The limit state function can be written as

$$Z = g(X_1, X_2, ...X_3) \tag{11}$$

Where, X_i represents probabilistically defined variables for the loads and the strength. The function g(-) is a limit-state function that characterizes the failure criterion. The probability function is then given by the joint probability distribution of $X_i's$

$$P_f = \int_{g(-)>0} \int f_{X_1 X_2 ... X_n.}(x_1 x_2 .... x_n) dx_1 dx_2 .... dx_n \quad (12)$$

Where, $f_{X_1 X_2 ... X_n.}(x_1 x_2 .... x_n)$ is the joint probability density function (pdf) of the random variables X_i. The evaluation of failure probability using efficient probabilistic analysis methods like First Order Reliability Method (FORM) is carried out by locating the most probable point (MPP) with a minimum number of model (function) evaluations. Whereas methods like Response Surface Method (RSM) employ the method for better approximation of limit state function.

A newly developed method Higher Order Response Surface Method (HORSM), which is based on higher order response surface approximation, approximates the true limit state function using Chebyshev polynomial as basis function $T_m(x)$ instead of regular polynomial $R_m(x)$. The Chebyshev polynomial and regular polynomial of order m can be given by $T_m(x) = \cos(m \cos^{-1}(x))$ and $R_m(x) = x^m$ respectively. The approximate LS of arbitrary order with $T(x)$ as basis function can be given as(2):

$$\hat{g}(\mathbf{X}) = a + \sum_{i=1}^{n} \sum_{j=1}^{k_i} b_{ij} \cos(j \cos^{-1}(X_i)) + \sum_{q=1}^{m} c_q \prod_{i=1}^{n} \cos(p_{iq} \cos^{-1}(X_i)) \quad (13)$$

where the coefficients b_{ij} correspond to uni-variate basis function, and the coefficients c_q correspond to multi-variate basis function. The polynomial order k_i, the total number of mixed terms m, and the order of a random variable in a mixed term p_{iq} are determined in the various stages of the proposed method. Details of the procedure are given in the [11]. The computational procedure for evaluation of implicit reliability levels are given below:

5.1 Fatigue Design Limit State Function

The limit state function $g(X)$ relates the expected accumulated damage ratio for the service life of a pipe D with the cumulative damage ratio that leads to failure D_f. When $g(X) \le 0$ the component fails, whereas when $g(X) \ge 0$ a safe design is assured. This can be shown mathematically using the (14).

$$g(X) = D_f - D \quad (14)$$

The expected accumulated damage D at a piping location is computed using the linear damage hypothesis proposed by Palmgren-Miner [12]. Then limit state function is given by (15).

$$g(X) = D_f - \sum_{i=1}^{nb} U_i = D_f - \sum_{i=1}^{nb} \frac{n_i}{N_{fi}} = D_f - \frac{n_{eqv}}{N_f} \quad (15)$$

where U_i is the usage factor at the i^{th} stress-range level, n_i is the expected number of cycles at the i^{th} stress-range level, N_{fi} is the number of cycles to failure at the i^{th} stress-range level, and n_b is the number of stress-range levels in a stress-range histogram, n_{eqv} is number of equivalent full temperature load cycles, and N_f is total number of cycles leading to failure. As discussed in the section-IV, the N_f depends on many variables. Therefore the limit state function can be written as (16) and (17).

$$g(X) = D_f - \frac{n_{eqv}}{N_f} = D_f - \frac{n_{eqv}}{f(A, S_a, F_{se}, F_{sf}, F_{en}, F_{def})} \quad (16)$$

$$g(X) = D_f - \frac{n_{eqv}(F_{se}.F_{sf}.F_{en})}{\exp\left(A - 1.920 \ln\left(\frac{Sa*100}{E} - 0.112\right)\right) F_{def}} \quad (17)$$

This is highly non-linear limit state function with eight random variables. Stochastic characteristics of these variables, except D_f, S_a, and n_{eqv}, are given in the section-IV and tabulated in the Table-II.

1) Cumulative damage ratio for failure (D_f)

   Although several cumulative damage laws have been proposed, yet the Miner's hypothesis of linear cumulative damage is a good assumption, when cycles of small and large stresses are evenly distributed throughout the piping service life. It is observed from the experiment under completely reversed loading condition on the un-notched geometries that loads having the larger stress cycles near the beginning of life tends to accelerate failure which leads to $D_f \le 1$. This is because cracks are initiated early in life and can propagate under lower stress amplitudes. However, if the smaller stresses are applied first and progressively higher stresses follow, the cumulative damage ratio for failure $D_f \ge 1$ [13]. Therefore, D_f in the design assessment stage is taken as random variable with a reasonable coefficient of variation of 0.10.

2) Equivalent number of full temperature cycle (n_{eqv})

   In practice component in NPP goes a range of temperature cycles in its useful life. It will be useful to convert the range of temperature cycles into an equivalent full temperature cycle, as per procedure similar to given for the ASME Class-2 piping. However, in this work, the maximum allowable no. of cycles permitted by ASME code

Table 2. Stochastic variables used for the failure probability estimation

S.N	Description	Mean	COV	Distribution
1	Constant –A from equation-5	6.891	0.061	Lognormal
2	Factor on life due to size effect (F_{se})	1.30	0.047	Lognormal
3	Factor on life due to surface finish (F_{sf})	2.68	0.17	Lognormal
4	Factor on life due to environmental effects (F_{en})	8.93	0.15	Lognormal
5	Factor on life due to conservatism in fatigue definition (F_{def})	2.0	0.1	Lognormal
6	Uncertainties in the cumulative Damage ratio variable (D_f)	1.0	0.10	Lognormal
7	Equivalent full temperature cycle (n_{eqv})	corresponding to S_a from FDC	0.1	Lognormal
8	Alternating stress intensity (S_a)	(S_p/2) -As per equation-2	0.10	Lognormal

corresponding to stress intensity is taken as mean value and a value of 0.1 as COV of the $n_{eqv.}$

3) Alternating stress intensity (S_a)

The alternating stress intensity S_a the is obtained as per procedure given in the section-II. Generally, the finite element analysis procedure is employed for estimation of stress intensity acting at various piping products and joints. This method requires mathematical modelling and discretization of its domain for response evaluation. Various uncertainties creep into the response evaluation while performing Integration of geometric properties, material properties and loads in the discretised domain and subsequent assembling for global response. Therefore, alternating stress intensity obtained from analysis is taken as mean value with uncertainties accounted by a COV of 0.10.

5.2. Computational Procedure

A computation procedure for evaluation of failure probability of class-2 nuclear pipeline is given by Avrithi and Ayyub [14]. A similar approach is taken for the computation of implicit reliability level of nuclear class-1 pipeline using (12). The steps in the evaluation procedure are as follows:

- Evaluate the alternating stress range, S_a corresponding to the cyclic loads.
- Evaluate the equivalent number of maximum temperature cycle, n_{eqv}. In the present case it is taken as number of cycles allowed by ASME fatigue design curve.
- Define limit state function using (17).
- Define the probabilistic characteristic of the variables used for defining the limit state function. These variables are $A, SR, SG, F_{def}, F_{en,nom}, D_f, n_{eqv}$ and S_a.
- Compute the failure probability, P_f and corresponding reliability index β using HORSM, FORM. The β represents the reliability index associated with code design procedure.
- Validate the result with Monte Carlo Simulation (MCS).

6. Computation of Implicit Reliability Levels

The reliability, which is complementary of the failure probability, is estimated using the three methods. The first method is FORM, which is very efficient in those cases where analytical expressions of the limit state function are available. Since in the present case the analytical expression is available, FORM is a useful tool for the failure probability estimation.

The second method is HORSM, which presume that limit state function in analytical form is not available. This method is especially suitable for the failure probability estimation of the actual NPP components, where limit state is evaluate using finite element analysis. Since in the present case limit state function is available, failure probability obtained from HORSM and FORM are matching closely. In those cases, where limit is not available in analytical form, HORSM give better estimate of failure probability. The MCS with $5x10^7$ iterations is used for the validation of the result obtained from FORM and HORSM method.

6.1 Sensitivity Analysis

The sensitivity of limit state function, $g(X)$ with respect to each variable is carried out by varying one variable at a time while keeping all other variables at their mean value. The variation is within one standard deviation from mean value. The sensitivity of the limit state function with

respect to variables in the normalised form is shown in the Fig. 4. It can be seen that the limit state function is most sensitive to cumulative damage ratio. The constant A and alternating stress intensity S_a also have high impact on limit state function. The variables for size effects and equivalent full temperature cycle have lesser effect on the variation of limit state function.

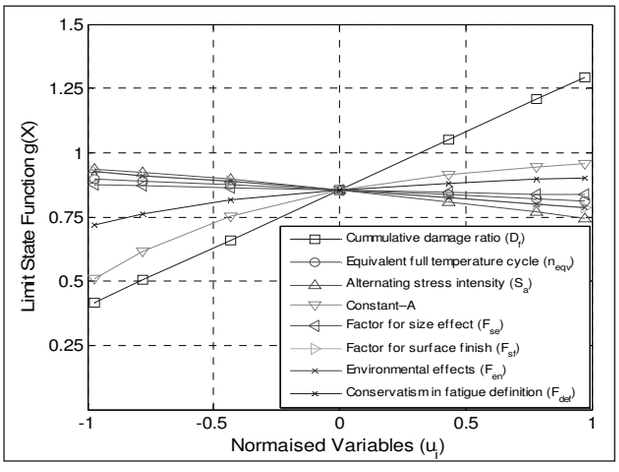

Fig. 4: Sensitivity of limit state function g(X) with normalized variables

$$(u_i = (x_i - \mu_i)/\sigma_i)$$

6.2 Failure Probability Evaluation

The failure probability of piping products and joints are estimated using FORM, HORSM and MCS. Two parametric studies are carried out to assess the variation of the failure probability with primary plus secondary stress range. For a typical case, a pipeline made up of austenitic steel SS304L and operating at 300°C, which is typically the operating temperature of the NPP reactors, is taken for failure probability evaluation.

1) Failure probability of butt welding elbow

The failure probabilities for butt welding elbow are evaluated for different value of primary plus secondary stress range, S_n. The S_n, is gradually varied from shakedown limit to twice of this limit, i.e. $3.0S_m$ to $6.0S_m$. Here, S_m is the maximum allowable stress intensity given in the ASME Section-II. The S_m value for the austenitic steel SS304L at 300°C is 98 MPa. When S_n is varies in this range of $3.0S_m$ to $6.0S_m$, the number of allowable fatigue life from ASME Section-III is in the range of 500 cycles to $4x10^5$ cycles.

The failure probabilities for elbow are given in the Table-III and Fig. 5. The values obtained from all three methods are nearly same. The failure probability is higher for butt welding elbow when number of allowable cycles is in the range of 1000-30000. The maximum value of the failure probability of ~$4.0x10^{-3}$ is observed when allowable number of cycles is in the range of 5000-10000. The corresponding S_n is nearly 1.25-1.35 times of Shakedown limit. It is also observed that when allowable number of cycles is 1000, which is generally the design criteria on no of cycles for pipelines, the failure probability is nearly ~$1.0x10^{-3}$. Beyond 10^5 cycles failure probability of the butt welding elbow t is fairly low.

2) Failure probability of piping products and joints

A parametric study is also carried out the compare the failure probabilities of the various pipe products and joints with respect to S_n. Five piping products like butt welding elbow, girth butt weld in the flush

Table 3 Failure probability of the class-I piping components Butt Welding Elbow, designed as per the ASME section-III.

S.N	Primary plus Secondary Stress	No. of Cycles from FDC of ASME	Failure Probability		
			HORSM	FORM	MCS
1	294.0	414060	1.00E-07	1.00E-07	6.01E-07
2	323.4	69486	7.05E-04	5.86E-04	4.95E-04
3	338.1	37584	2.35E-03	2.52E-03	2.25E-03
4	352.8	21575	5.14E-03	5.04E-03	4.58E-03
5	382.2	8777	9.69E-03	8.98E-03	8.36E-03
6	411.6	4014	8.85E-03	7.67E-03	7.22E-03
7	441.0	2023	4.89E-03	4.84E-03	4.64E-03
8	470.4	1175	4.10E-03	3.62E-03	3.43E-03
9	499.8	749	3.16E-03	3.03E-03	2.89E-03
10	543.9	602	2.98E-03	2.82E-03	2.66E-03
11	588.0	493	2.84E-03	2.60E-03	2.46E-03

and as-welded condition, longitudinal butt weld in the as-welded condition and branch connection are taken for the comparison. The S_n is gradually varied from half of the shakedown limit to twice of this limit i.e. $1.5S_m$ to $6.0S_m$. The results are plotted in the Fig. 6, with X-axis representing the stress range S_n in the normalised form.

It is observed from this figure that for the piping product with higher value of peak stress indices, K_2

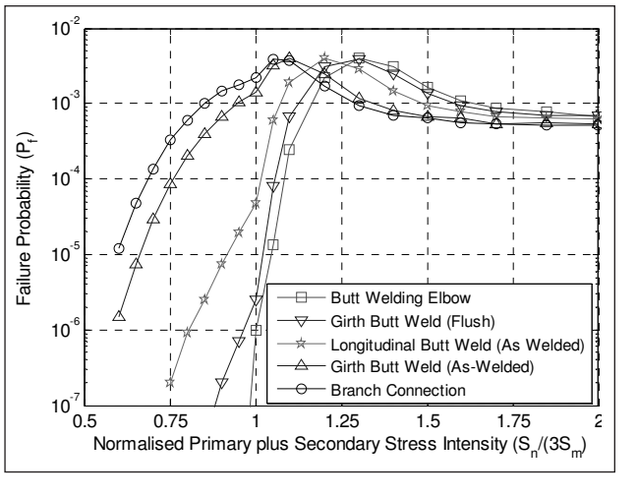

Fig. 6: Reliability index of class-I components designed as per class-III with respect to primary plus secondary stress intensity (Sn)

the curve shift towards left inferring that failure will occur at the lower value of S_n. At the shakedown limit the failure probability evaluated for butt welding elbow, girth butt weld (flushed), longitudinal butt weld (as-welded), girth butt weld (as-welded), and branch connection are $1.0x10^{-6}$, $2.5x10^{-6}$, $4.7x10^{-5}$, $1.4x10^{-3}$, $2.2x10^{-3}$ respectively. This shows that failure probability of branch connection is three orders higher than butt welding elbow. However, for piping products and joints with same value of peak stress indices, K_2 like straight pipe, butt welding elbows, butt welding tees, the failure probabilities at the shakedown limits will be same.

7. Conclusion

The paper describes a procedure to estimate the implicit reliability level associated with the fatigue design criteria of class-1 piping specified by ASME BPV Code, Section III, NB-3650. The reliability evaluation is carried out using mean fatigue curve given by ANL because it matches closely with ASME fatigue design curve when a factor of 2 on stress and 12 on life is applied on them. Limit state function for reliability evaluation, which is based on linear damage hypothesis proposed by Palmgren-Miner, is developed using eight parameters affecting the fatigue life. The sensitivity analysis of the limit state function suggests that it is strongly sensitive to cumulative damage ratio, constant-A of fatigue mean curve and alternating stress intensity, whereas geometry (size) and equivalent temperature cycle have less predominant effect.

It is observed that the failure probability of butt welding elbow due to fatigue is higher when number of allowable cycles is in the range of 1000-30000. The maximum value of the failure probability of ~$4.0x10^{-2}$ is observed when allowable number of cycles is in the range of 5000-10000. The corresponding S_n is nearly 1.25-1.35 times of Shakedown limit. Also, the failure probability is lower for those pipe products and joints which have higher value of peak stress indices. Due to this reason failure probability of branch connection is three orders higher than those of butt welding elbow. Therefore it is concluded that the failure probabilities of piping products and joints of pipeline, which is designed as per ASME Section-III fatigue design criteria, will have large variations.

Nomenclature	
a	Constant term of polynomial
A,B,C	Constants of Langer equation
b_{ij}	Coefficients of uni-variate basis function
C_q	Coefficients of multi-variate basis function
C_1,C_2	Secondary stress indices for the specific component under investigation
D	Expected accumulated damage ratio for the service life
D_0	Outside diameter of pipe
D_f	Cumulative damage ratio that leads to failure
$f_{X_{1,..,n}}(x_1,..,x_n)$	Joint probability density function of the random variables X_i
$F_{en,nom}$	Nominal environmental fatigue correction factor
F_{en}	Factor on life due to environmental effects
F_{se}	Factor on life due to size effect
F_{sf}	Factor on life due to surface finish
F_{def}	Factor on life due to conservatism in fatigue definition
$g(X)$	Limit state function
I	Moment of inertia

K_1, K_2	Peak stress indices
m,n	Material parameters
M_i	Resultant moment due to a combination of design mechanical loads
nb	Number of stress-range levels
n_{eqv}	Number of equivalent full temperature load cycles
$N_{air,RT}$	Number cycle to failure in the air environment
N_f	Fatigue life or total number of cycles to failure
N_{fi}	No. of cycles to failure in i^{th} stress-range level
N_{water}	Fatigue life in the water at service temperature
O'	Transformed DO levels
P_0	Range of service pressure
P_f	Failure probability
$R_m(x)$	Regular polynomial
S_a	Alternating stress intensity
S_m	Allowable stress intensity value of the metal
S_n	primary plus secondary stress intensity value
S_p	Peak stress intensity value
T'	Transformed temperature
t	Nominal wall thickness of product
$T_m(x)$	Chebyshev polynomial
U_i	Usage factor at the i^{th} stress-range level
X_i	Random variables
Z	Section Modulus
ε_a	Alternating strain amplitude
$\dot{\varepsilon}'$	Transformed strain rate

References

1. American Society of Mechanical Engineers (ASME), Rules for construction of nuclear facility components, ASME Boiler & Pressure Vessel Code, 2010.
2. Gupta, A., Choi, B., Reliability-based load and resistance factor design for piping: An exploratory case study, Nuclear Engineering and Design 224, 161- 178, 2003.

3]. Ralph S. Hill III, Probabilistic & System - based Methods for design - development of reliability-based load and resistance factor design methods for piping, ASME Nuclear Codes and Standards Workshop, New Orleans, LA, 2004

4. American Society of Mechanical Engineers, Rules for construction of nuclear facility components, ASME Boiler and Pressure Vessel Code, Section-III , Appendix-I, 2010.
5. Rodabaugh, E. C., Comparisons of ASME Code Fatigue Evaluation Methods For Nuclear Class 1 Piping with Class 2 Or 3 Piping, NUREG/CR-3243, 1983.
6. Langer, B. F., Design of Pressure Vessels for Low–Cycle Fatigue, ASME J. Basic Eng. 84, 389–402, 1962
7. Chopra, O. K., and Shack, W. J., Effect of LWR Coolant Environments on the Fatigue Life of Reactor Materials-Final Report, NUREG/CR-6909 and ANL-06/08, 2007
8. Chopra, O. K., Mechanism and estimation of fatigue crack initiation in austenitic stainless steels in LWR environments, NUREG/CR-6787, 2002.
9. Chopra, O. K., and W. J. Shack, Review of the Margins for ASME Code Design Curves - Effects of Surface Roughness and Material Variability, NUREG/CR–6815, ANL–02/39, Sept. 2003
10. Chopra, O. K., and W. J. Shack, Environmental Effects on Fatigue Crack Initiation in Piping and Pressure Vessel Steels, NUREG/CR–6717, ANL–00/27, May 2001
11. Mishra, J. , Chellapandi, P , MeherPrasad, A. , Narayanan S., Evaluation of Failure Probability of Expansion Bellow at RCB Containment Penetration of PFBR using Higher Order Response Surface Method; SRESA International journal of Life Cycle Reliability and Safety Engineering, Vol.3, Issue No.-2, PP-15-24, 2014
12. Miner, M. A., Cumulative Damage in Fatigue, J. Applied Mechanics, 12, A159-A164, 1945
13. Fatemi, A.,Yang, L., Cumulative fatigue damage and life prediction theories: a survey of the state of the art for homogeneous materials, Int. J. Fatigue, Vol. 20, No. 1, pp. 9-34, 1998
14. Avrithi, K., and Ayyub, B. M., A Reliability-Based Approach for Low-Cycle Fatigue Design of Class 2 and 3 Nuclear Piping, Journal of Pressure Vessel Technology, Vol. 132, 2010

Life Cycle Reliability and Safety Engineering
Vol.5 Issue 1 (2016) 18-28

Maintenance Imperfection Centered Performance Management Framework

Monika Tanwar, Nomesh Bolia
Department of Mechanical Engineering, Indian Institute of Technology, Hauz Khas, New Delhi-110016, India
Email: monika.tanwar79@gmail.com

Abstract

Maintenance management (MM) effectiveness depends on corporate strategies as well as maintenance policies. The purpose of this paper is to provide a generalized methodical approach of maintenance performance management (MPM), incorporating the strategic, tactical and operational aspects of maintenance performance while considering interactions of its key elements. Men, machine, material, method, measurement and environment are considered key elements of any maintenance action to perform satisfactorily. A MPM framework is developed taking imperfect maintenance into account to attain the required output. The work is devoted to two major parts of MPM, i.e. defining maintenance strategy and the implementation process for maintenance management.

Keywords*: Repairable Systems, Imperfect Maintenance, Maintenance Performance, FECA*

Notations and Abbreviations

C	Scale value of Factor Criticality
FECA	Factor Effect Criticality Analysis
FMEA	Failure Mode and Effects Analysis
GRP	Generalized Renewal Process
MLE	Max. Likelihood Estimator
MM	Maintenance management
MPM	Maintenance Performance Management
NHPP	Non Homogenous Poisson Process
O	Scale value of Probability of failure occurrence
p	Probability of failure occurrence
q	Maintenance imperfection index
Q	Scale value of Maintenance Imperfection
RAM	Reliability, Availability and Maintainability
RP	Renewal Process
RPN	Risk Priority Number
TMM	Total Maintenance Management
TPM	Total Productive Maintenance
TQM	Total Quality Maintenance
v_n	Virtual Age at n
x_n	Time between failure
α	Characteristic Life
β	Shape Parameter

1. Introduction

Maintenance is defined as an effort to retain operability of an item utilizing maintenance resources under defined policies, and schedules within required time frame. MM deals with numerous activities to achieve its intended goal and managing assets. The main aspects of MM are (Marquez, 2007): maintenance objective identification, strategies formulation, strategy implementation, and improvement in methodologies. The golden era for maintenance has started, as the focus is turning towards proactive maintenance from reactive maintenance ("unnecessary evil") and MM is emerging as an indispensable part of business management rather than a section targeted for cost cutting. A literature review that demonstrates this is presented next. Simoes et al. (2011), in their detailed review, classify and analyze three decades i.e. 1979 to 2009 of research in MM and maintenance performance measurement. The research interest in the field is growing. MM now has a significant literature support based on performance indicators, development of performance frameworks and management. The review has been conducted focusing on related aspects like three levels of management i.e. strategic, tactical, and operational; maintenance strategy development, and MM over last fifteen years. The available literature can be broadly classified into MM framework and maintenance performance measurement.

1.1 MM Framework

The control board approach (Pintelon & Wassenhove, 1990) proposes sets of performance indicators in terms of effectiveness ratios related to different sections of MM and also provides a MM tool. The authors reject the approach of the use of single overall performance measurement index mentioning the risk of obscurity of data. Pintelon and Gelders (1992) present an insight on MM decision making in a structural format. They elaborate the MM evolution as a business function, and describe maintenance system design aspects, decision making and provide a managerial tool kit. Raouf (1993) discusses limitations of maintenance cost ratio as a measurement for benchmarking and thus develops total maintenance cost standards which include maintenance sub-function costs. The study by Jostes & Helms (1994) presents the need of integration of Total Productive Maintenance (TPM) and Total Quality Maintenance (TQM) for competing manufacturing industries. Raouf and Ben-Daya (1995) develop a systematic approach towards total maintenance management (TMM) comprising of MM, maintenance operations, and equipment management. The practical approach of Groote (1995) suggests a solution for existing maintenance problems from organizational and operational point of view taking audit as a powerful tool for analysis with Sherwin and Jonsson (1995) present the need of interprets maintenance with production planning and control. Swanson (1997) provides the empirical relation between production technology and MM by studying the various aspects of both the sections. Maintenance as a tactical level issue is discussed in detail for its strategic importance by Tsang (1998). Tsang et al. (1999) further extend the work by identifying linkage between strategic and tactical level management using balance score card (BSC). The authors use Data Envelopment Analysis for benchmarking the BSC practicing organization.

1.2 Maintenance Performance Measurement

A detailed literature survey (Neely, 1999) attempts to answer why performance measurement has become an important issue. Neely et al. (2000) explain how the existing tools such as BSC and performance prism can be populated and business specific performance indicators can be selected. Kutucuoglu et al. (2001) analyse the importance of a performance measurement system (PMS) in maintenance and identify the key performance factors to develop PMS using the quality function deployment technique. Swanson (2001) identifies the relation between maintenance strategy and maintenance performance under TPM with preventive, predictive and aggressive maintenance strategies. Murthy et al. (2002) bring out the importance of strategic aspect of maintenance with its operational efficiency. Visser (2003) defines maintenance performance and measures, and manages to achieve production aims considering system condition and safety. Marquez & Gupta (2006) discuss MM process, framework and supporting pillars i.e. pillars of information technology and maintenance engineering. Pinjala et al. (2006) present empirical results of surveys conducted in 150 manufacturing companies to find relation in maintenance objectives and business strategies over quality competition. Parida and Kumar (2006) summarize issues and challenges related to maintenance performance measurement. Parida (2007) provides a multi-criteria view to maintenance performance measurement and defines related performance indicators in a balance score card approach. A CIBOCOF framework and case study is presented to describe the structural development of maintenance concept for a specific industry Waeyenbergh (2009). Muchiri et al. (2011) provide maintenance performance framework with various leading and lagging maintenance performance indicators considering strategic level MM. Another detailed review (Kumar et al., 2013) in the area of performance measurement presents a view to get compatibility of maintenance strategy and performance measurement technique. An ANP approach is used for selection of business specific MPI among available MPIs and maintenance performance measurement is proposed by Horenbeek & Pintelon (2014).

Summarizing the literature it has been observed that maintenance performance measurement, performance indicators, MM, and maintenance strategies are well researched and developed using various tools like BSC, CIBOCOF, RCM (Reliability Centered Maintenance), TPM, and TQM etc. The generalized research gaps identified from literature review are listed in Table 1.

This paper proposes a MPM framework that addresses the research gaps listed in Table 1. Three sections of MPM i.e. strategic, tactical and operational level are discussed in detail. For maintenance performance measurement, a diverse phenomenon of imperfect maintenance is used. It has been proven that maintenance may often not be able to reinstate the system operating condition to as good as new i.e.

Table 1: Research gaps from literature

Sr. No.	Research Gaps
1.	Lack of MPM Models
2.	Need of operative methodology of general applicability
3.	Lack of plant/process knowledge and data
4.	Lack of analysis time
5.	Large number of maintenance performance indicators, need of business specific MPI, monitoring or measurement all of the available indicators is not feasible
6.	Limited Literature incorporating all three levels of management
7.	Deriving MPI for maintenance objectives
8.	No methodology for transformation of business objective to maintenance objective
9.	Unavailability of single overall performance measurement index mentioning the risk of obscure of data
10.	Need for flexible maintenance concept allowing feedback and improvement
11.	Practical implementation feasibility
12.	Framework structure complexity
13.	Dynamic maintenance performance approach
14.	Imperfection in maintenance is not considered

condition at the beginning of operation (Kijima, 1989). Literature reviews (Wang & Pham, 1996; Tanwar et al. 2014) for imperfect maintenance modeling supports the existence of this phenomenon. Therefore if the maintenance is imperfect than its management requires consideration of imperfect maintenance in designing the MPM framework. The behavior based maintenance is also considered an integral part of

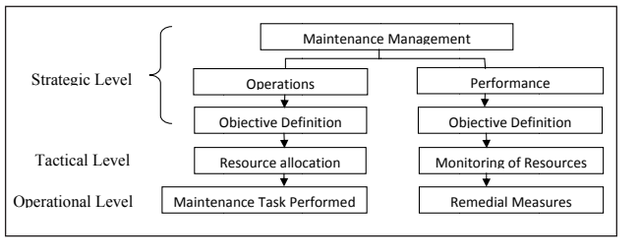

Fig 1: Maintenance Management Levels

object/ objective oriented maintenance management by Zhu et al. (2002). Fig 1 presents the broad outline of MM.

MM broadly deals with operations management and performance management for an overall management. In general MM largely focuses on operations management to complete assigned task satisfactorily. In recent times maintenance performance measurement has gained momentum. Though researchers have described various maintenance performance indicators in general and also specific to business, the research is still lacking a maintenance performance management framework considering all three levels of management and measured performance indicators. This paper focuses on one such framework and is discussed in detail in the following sections: section 2 describes imperfect maintenance in MPM and illustrates the framework developed for three levels of MPM; section 3 discusses MPM performance matrix; section 4 provides contribution made by proposed approach and concludes the work.

2. Role of Imperfect Maintenance in MPM

System and components are widely considered as repairable and non-repairable. System at large is considered repairable as it may comprise numerous sub-systems and components, those can be either repairable or non- repairable. The basic consideration for repairable and non-repairable component is: on failure, non-repairable component is replaced with identically new or working component whereas the repairable component is repaired to restore its operating condition. Therefore application of similar mathematical models for maintenance modelling of repairable and non- repairable systems, does not justify the actual practice. It is observed that RP and NHPP are extensively used mathematical models for non-repairable as well as for repairable systems but GRP is widely used only to model repairable systems. Various (p,q), (α,β) rules and Kijima virtual age models etc. (Wang & Pham, 1996; Tanwar et al., 2014) are available in the literature for repairable system modelling. These models discuss the concept of "repair effectiveness or imperfect maintenance". Imperfect maintenance refers to an intermediate after-repair state other than the perfect repair (as good as new). These intermediate states have possibilities of 'as bad as old', 'better than old worse than new', and 'worse than old' after-repair states. A maintenance imperfection index q is well defined in literature (Kijima, 1989) to quantify these intermediate states or the extent of imperfection in maintenance through virtual age models. Kijima I virtual age model is defined as:

$$v_n = q\sum_{i=1}^{n} x_i \qquad (1)$$

According to Kijima-II model the repair action at any point of time restores the entire accumulated age since new and is given by:

$$v_n = qx_n + q\sum_{i=1}^{n-1} q^{n-i} x_i \quad (2)$$

where v_n is the virtual age after n^{th} failure; x_n is the time between failure in n^{th} and $(n-1)^{th}$ failure; x_i is the time between i^{th} and $(i-1)^{th}$ failure and q is the repair effectiveness index. Parameters estimation using numerical solution to MLEs, and expected number of failures are provided in detail by Yanez et al. (2002). It has been observed that the lower value of maintenance imperfection index shows better effect of maintenance, as moving close to 'as good as new' state. The reduction in maintenance imperfection index value can be attained or controlled by maintenance management. There can be various reasons for imperfection in maintenance as the maintenance activities are performed with the support of numerous sub-activities of maintenance and the available literature helps to identify those reasons (Dhillon and Liu, 2006; Bloch & Geitner, 1999; Matthews, 1998; T. Tinga, 2013; Daydem, 2005). Therefore, to understand the role of imperfection in MM at various levels of management, a study is conducted and discussed in detail in the next section. MM framework is then drawn at different levels of management, with an aim of reduction of imperfection in maintenance.

2.1 Strategic Level MPM

At this level the organizational management and MM synchronize to identify the maintenance objective. The organizational aims are transformed into maintenance objectives. A generalized maintenance scenario is considered where user manages maintenance as per equipment condition and the maintenance guidelines provided by manufacturer or vendor. Under this scenario the user is responsible for overall equipment maintenance using internal resources and vendor maintenance support. The aviation maintenance, railway maintenance, and military maintenance are few examples under the defined scenario. System reliability, availability and maintainability (RAM) are acknowledged as organizational technical objectives in most of the organizations (Sharma & Kumar, 2008; Eti et al., 2007; Zerwick, 1995; Carlier, 1996; Ebling, 2007) and the importance of RAM characteristics is discussed in detail in the US defence document (DOD, 2005). Improvement in RAM characteristics further can produce profit, growth, and social aims for any organization. These organizational technical objectives (RAM) need to be transformed into a technical maintenance objective. There are numerous aspects like design of system, operating environment, maintenance scheduling, planning, optimization, and human error etc. that can affect RAM characteristics of system and can be targeted for improvisation. For MM, factors related to maintenance need to be focused. The maintenance factors affecting RAM of system, individually cannot define an overall maintenance objective. Therefore need for a technical performance parameter is felt which can reflect an overall maintenance effort. The other maintenance objectives such as financial objectives, legal objectives, and safety are out of scope of the work.In this work the imperfect maintenance index is studied for its aptness as quantitative measure for technical maintenance objective. The analysis is performed on maintenance imperfection. Failures affect the organizational targets i.e. system reliability, availability and maintainability consequently (Ebling, 2007). A sensitivity analysis is discussed to provide an insight on dependence of various failure parameters on maintenance imperfection. It is observed that detailed sensitivity analyses present in literature (Jacopino et al., 2004; Yu et al., 2013) can provide a good base to the strategy selection. Jacopino et al., (2004) describe the failure distribution parameters i.e. shape parameter, scale parameter and expected number of failures variations with respect to maintenance imperfection index. Work by Yu et al. (Yu et al., 2013) shows that repair effectiveness significantly affects number of failures and also checks whether the current repair effectiveness can meet the targeted reliability or not. A sensitivity analysis carried out by Rai & Bolia (2014) presents variations of conditional probability of failure versus q. The authors also provide the improved organizational objectives through improvement in q for different failure modes. Therefore to achieve system reliability, availability and maintainability as organizational aims sensitivity analysis justifies the selection of imperfect maintenance as maintenance objective at strategic level. Fig 2 shows predicted number of failures for different values of q. The exponential rise in failure arrivals can be observed with increased imperfection. Fig 3 to 6 present expected number of failures verses time to failures. Kijima I and II (Kijima, 1989) models are simulated with varying q and β. It is observed that with constant β value and increasing q value, expected number of failures increase rapidly for both the virtual age models. Further with constant q and varying β value shows variations in number of failures which indicate that maintenance organization cannot work with a constant maintenance concept if

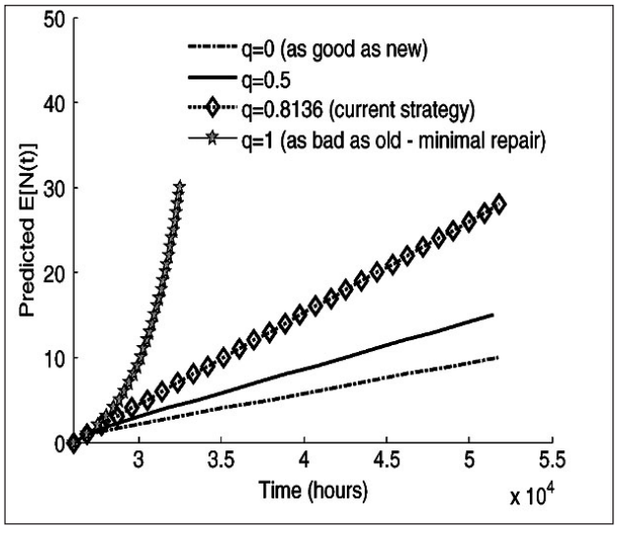

Fig. 2: Predicted future number of failures with different values of q (Yu et al., 2013)

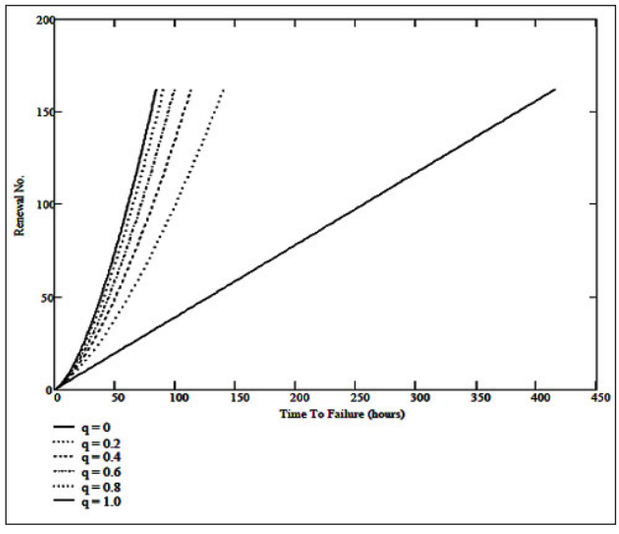

Fig 3: Simulated Kijima Type I model (β=1.5, q=0, 0.2, 0.4, 0.6, 0.8, 1; Jacopino et al., 2004)

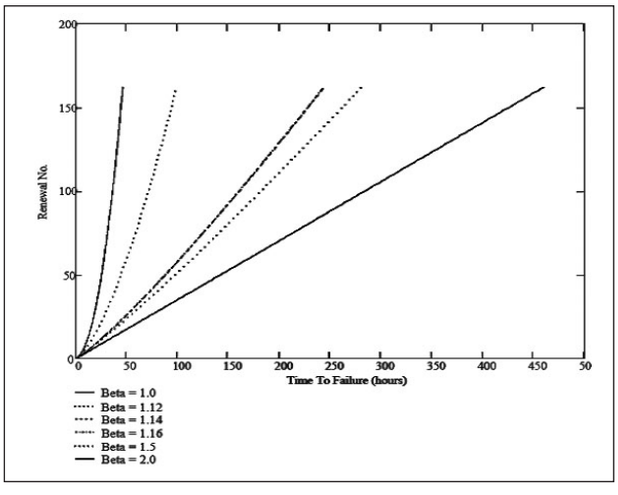

Fig 4:Simulated Kijima Type I model (q=0.6, β=1, 1.12, 1.16, 1.2, 1.5, 2); (Jacopino et al., 2004)

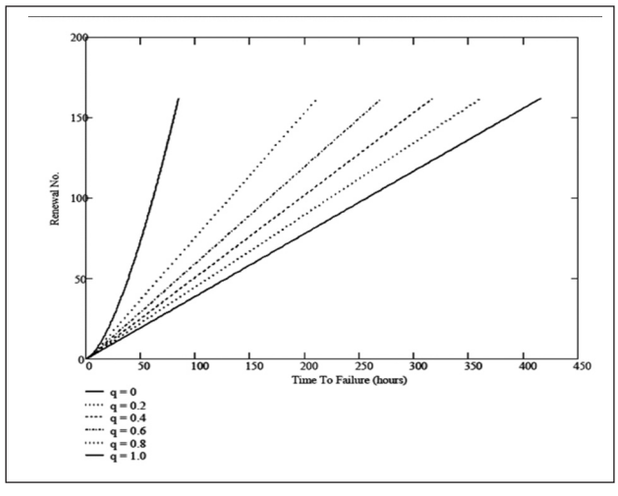

Fig 5: Simulated Kijima Type II model (β=1.5, q=0, 0.2, 0.4, 0.6, 0.8, 1); (Jacopino et al., 2004)

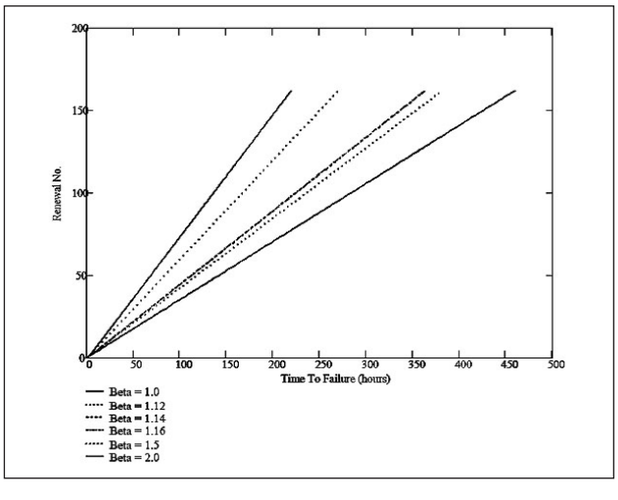

Fig 6: Simulated Kijima Type II model (q=0.6, β=1,1.12,1.16,1.2,1.5,2; (Jacopino et al., 2004)

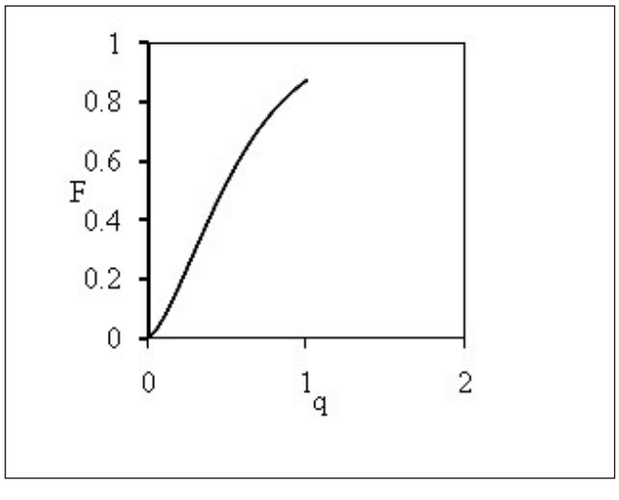

Fig 7: q Vs F ($V_i \mid V_{i-1}$) for FM1 (Rai & Bolia, 2014)

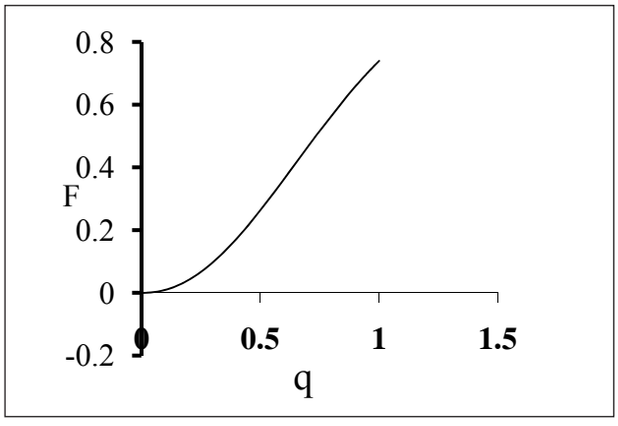

Fig 8: q vs. F (Vi/V_{i-1}) for FM2 (Rai & Bolia, 2014)

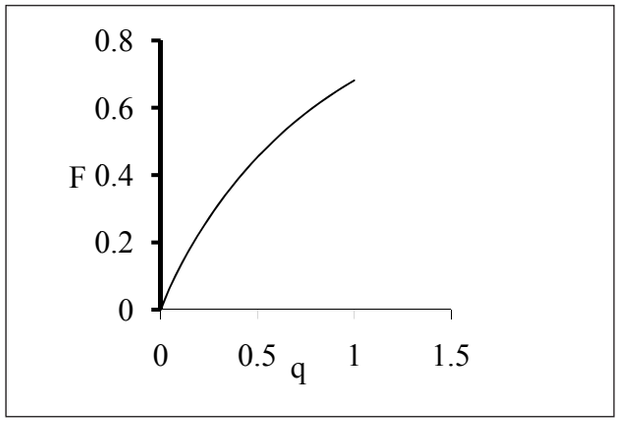

Fig 9: q Vs F ($V_i \mid V_{i-1}$) for FM3 (Rai & Bolia, 2014)

the equipment is ageing with time and maintenance imperfection index q can be a controlling parameter for desired expected number of failures. Fig 7 to 9 show the conditional probability of failure variations with q for three different failure modes (FM), representing q as a controlling parameter.

To reduce the maintenance imperfection, tactical level management is studied in next section.

2.2 Tactical level MPM

Fulfillment of maintenance objective in tactical mode requires correct allocation of maintenance resources (skills, materials, test equipment etc.), chalking out a detailed program with all the specified tasks and assigned resources for operations MM.

It is recalled that we are dealing with MPM and maintenance imperfection reduction is the objective identified to be achieved. It necessities identification of factors responsible for maintenance imperfection as well as individual factor performance measurement and their contribution in causing maintenance imperfection. To identify factors responsible for maintenance imperfection, the literature (conceptual and work studies) is studied and discussed. Problems that occurred in learning from the causes of the incidents or failures are studied for seven cases (Drupsteen & Hasle, 2014) and it is observed that there is a need of "learning to learn" to check learning process bottlenecks. Human errors are specific to the type of maintenance system or organization e.g. manufacturing plant maintenance, power plant maintenance, aviation maintenance and rail transportation maintenance etc., and these system specific errors are discussed, (Dhillon and Liu, 2006); (Latorella & Prabhu, 2000) where authors present brief reviews on human errors in aviation industry,

Table 2: Maintenance imperfection factors categorization

Sr. No.	Categories	Description
1	Men	Human errors that resulted in failures and delays at any level of management
2	Machine / Technology	Equipment or technology on which the maintenance action is performed and equipment ageing
3	Material	Supporting tools, spare parts, consumables, raw material etc.
4	Method	Discrepancies due to process, schedules, policies, procedures, rules, regulations and laws related to every section of management
5	Measurement	Error in data generation, collection, observation and analysis
6	Environment	Operating conditions, such as location, time, temperature, work load etc. responsible for failure

nuclear power sector, chemical processing, medical device, mining and various other maintenance fields. Failures related to material and machine/technology are widely discussed by authors (Bloch & Geitner, 1999; Matthews, 1998). A detailed analysis of failure modes of aero engine and their effects (Rai & Bolia,

2014) summarizes the numerous failure causes those broadly cover the categories of men, machine, material, method, measurement and environment. The authors provide guidelines for failure modes and failure mechanisms which further helps in selection of imperfection factors (T. Tinga, 2013; Daydem, 2005). The need of maintenance resources management is described in detail by Kelly (2006). After compiling factors as an outcome of performance failures responsible for imperfect maintenance, it is observed that each cause or reason for imperfection is a source of variation. These causes can be grouped into six major categories to identify the sources of variation. The selected categories cover all aspects, sections and levels of MPM that can generate imperfection. The categories typically include:

A cause and effect diagram is used to present

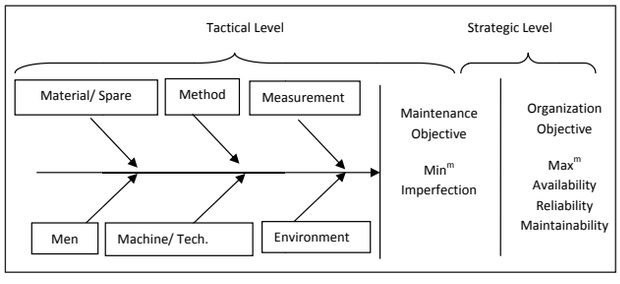

Fig 10: Strategic and Tactical level Maintenance Performance Management Diagram

the link between the imperfection causes and effect. Fig 10 shows the strategic and tactical level of MPM framework.

The next section proposes the framework of operational level of MPM.

2.3 Operational level MPM

At operational level of maintenance management, the maintenance tasks are carried out by skilled technicians, in the scheduled time following the correct procedures using the proper tools.The operational level of MPM ensures the imperfection control by carrying out tasks satisfactorily, collecting failure and error data for information system and further analyzing data. The data should be capable enough to capture the imperfection contribution. Note that the corrective measures for a system's failure now become a critical function. This task requires involvement of specialists and uses complex technological tools and measures. Hence, the troubleshooting process depends closely on the maintenance information system that provide information about all the work done on each piece of equipment. Fig 11 presents the operational level networking of all imperfection causing factors.

The complex networking shows that each factor has operational connection to remaining all factors. MPM structure proposes the sequence of steps to practice in order to manage maintenance performance accurately. Maintenance operations management framework in general is comprised of building blocks of different sections of management, e.g. maintenance objective and strategy formulation, assets management, maintenance policy design, scheduling and optimization, life cycle analysis etc. These building blocks are further dealt with using various analytical

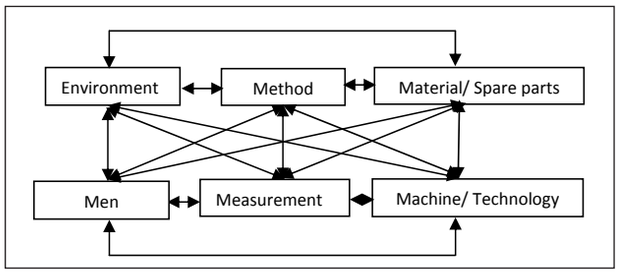

Fig 11: Operational level networking of key maintenance factors

models such as balance score card, criticality analysis, failure root cause analysis, reliability cantered maintenance, risk–cost optimization and life cycle cost analysis respectively.

The use of specific tools for individual management building block performance analysis seems a complex structure. An overall performance measurement based on performances of these blocks is a rigorous task. Selection of six factors at tactical level of management makes it possible in a comparatively effective manner, as factors selected at tactical level of MPM caters at each building block of operations management.

Fig 12 presents the features of operational level process of MPM. If management is able to diagnose the errors correctly, any maintenance organization can provide better results with the proposed framework. It has system operation as starting point and next is occurrence of failures, the data reporting starts for failure time, failure type, possible failure mode etc. Overall failure parameters are estimated. Failures are further analyzed for its causes using any of available analytical tools i.e. logic tree analysis (LTA), root cause analysis (RCA) in the organization. The analysis results into cause identification and the cause removal. The system gets restored after cause removal, and is sent back to operation. Cause identification is fed into classification for imperfection contribution

factors. Failures related to each factor are recorded under respective categories. Failure parameters (shape parameter, scale parameter and imperfect maintenance index) are then estimated for each factor category. Estimated parameters reflect the operating state of factors in the maintenance organization. Sensitivity analysis of factors with respect to imperfect maintenance index then presents the improvement scope in imperfection index by improving factor performance or shows the extent of effort required to improve performance for a required imperfection

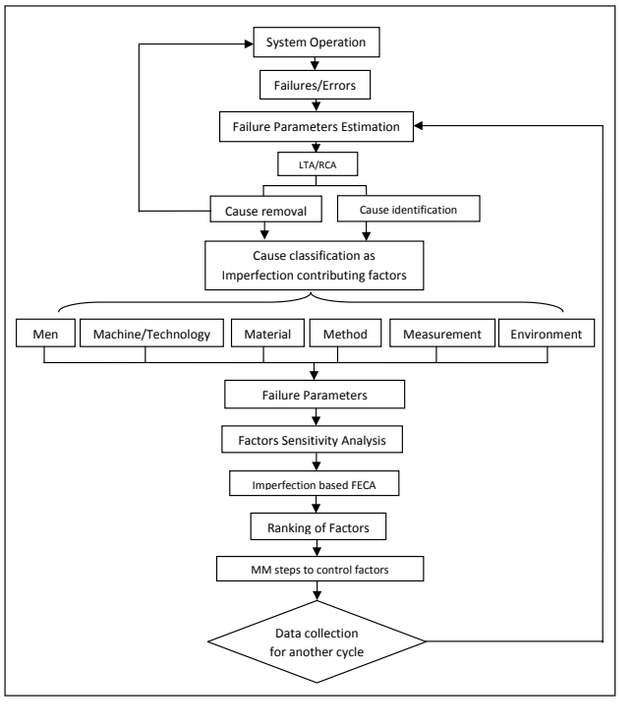

Fig. 12: Operational level process for maintenance management

index. Further an imperfection based factor effect criticality analysis (FECA) is conducted to rank the factors. The imperfection based FECA is explained in next section. For higher ranking factors, remedial measures can be taken by the management.

3. Imperfection based FECA

Factor Effect and Criticality Analysis (FECA) is a modification of existing Failure Mode Effect and Criticality Analysis (FMECA) which is an analytical tool used in charting the selected factors against the maintenance imperfection caused as their effect. Fig 13 depicts the imperfection based FECA, in which scaled values of probability of occurrence (O) is along the ordinate and scaled value of imperfect maintenance index (Q), is on the abscissa. The criticality of specific factor for the maintenance organization is denoted by C.

3.1 Probability of occurrence

The probability of occurrence is estimated for the factor is based on estimation of expected number of failures as given by Yanez et al. (2002) using Monte Carlo simulation. For first failure the Cdf is given by Yanez et al. (2002)

$$F(t)=1-\exp\left(-\frac{t}{\alpha}\right)^{\beta} \quad (3)$$

For subsequent failures:

$$F(t_i)=1-\exp\left[\left(\frac{q}{\alpha}\sum_{j=1}^{i-1}t_j\right)^{\beta}-\left(\frac{t_i+q\sum_{j=1}^{i-1}t_j}{\alpha}\right)^{\beta}\right] \quad (4)$$

The probability of occurrence for factors is then grouped into qualitative range (Ebeling, 2007):

Level A: Frequent (p>=.0.2)

Level B: Probable (0.1≤ p≤0.2)

Level C: Occasional (0.01≤p≤0.1)

Level D: Remote (0.001≤p≤0.01)

Level E: Extremely Unlikely (p<0.001)

The rating is done on a 10 point scale, e.g. Level A is rated as 10 and E as 1 (Rai & Bolia, 2014).

3.2 Imperfect Maintenance Index

The maintenance imperfection index is estimated using Kijima I model (Kijima, 1989; Yanez et al., 2002). The imperfection parameter q is estimated solving MLEs (Yanez et al., 2002), the values are further scaled for FECA. Table 3 present the scale value for probability of occurrence, imperfect maintenance index and factor criticality respectively.

Table 3: Imperfect Maintenance Index Scale

Scale Value (Q)	Imperfect Maintenance Description
1-8	Better than old worse than new
9	As bad as old
10	Worse than old

3.3 Criticality

Criticality of selected factors can be estimated on the basis of expert judgment and deciding on factor importance for specific maintenance organization. Factor criticality for a maintenance organization

Table 4: Factor Criticality Scale

Criticality Level (C)	Very High	High	Moderate	Low	Very Low
Scale Value	5	4	3	2	1

depend on organization goal, policies, system set-up etc. All selected factors can be scaled on factor criticality scale as shown in Table 4.

The FECA matrix is then drawn and the locations for all selected factors are presented as M1, M2, M3, M4, M5 and E, for men, machine, material, method, measurement and environment respectively and are marked as illustration to complete the MM performance matrix in Fig 13.

The RPN value ranges from 1 to 500. The risk priority number (RPN) is given by:

$$RPN = O \times Q \times C \quad (5)$$

Various locations in FECA indicate the performance level of selected factors. Location A indicates that the factor is performing satisfactorily, causing lowest value of imperfection. Location B depicts lowest probability of failure occurrence but highest imperfection contribution, a critical situation if encountered as indicating factor is in bad shape, depreciating, ageing, bad operating conditions, wrong measurements etc. Location C represents performance is satisfactory if factor is not critical. Location D indicates high failures with low imperfection contribution, which representing missing data in parameter estimation. Location E is the most attention required location representing worst performance of factor with highest probability of failure occurrence and highest imperfection contribution.

Q / O	1	2	3	4	5	6	7	8	9	10
1	A									B
2										
3							M1			
4										
5					C					
6						M2			E	
7								M3		
8					M4					
9							M5			
10	D									E

Fig 13: Imperfection based FEA: MPM Matrix

The remedial measures will depend upon the factor to be improved.

Conclusion

There is a lack in research in arriving at effective maintenance strategies for maintenance performance measurement and management. However, the research is more devoted towards operations part of maintenance management and is lacking in performance management. This leads to application of inappropriate strategies at times. In this paper the MPM framework is derived for all three levels considering maintenance imperfection reduction as an objective to achieve organization's technical objective i.e. system reliability, availability and maintainability. The Ishikawa cause effect diagram is used to identify causes of imperfection. Men, machine/technology, material, method, measurement and environment are identified as key factors responsible for maintenance management. Further the operational level management presents the implementation framework with the MM performance matrix. Individual factorscan be studied in detail for their imperfect maintenance contribution and analysis can be carried out for their interlinking. The work can be extended by analysis in more detail the linkages of the operational level networking of key maintenance factors.

References

1. Bloch, H.P. and Geitner F.K., "Machinery Failure analysis and Troubleshooting", Gulf Publishing Company,Houston, Texas, USA, 1999.
2. Carlier, S., Coindoz M., Deneuville, Garbellini, and Altavilla A.,"Evaluation of reliability, availability, maintainability and safety requirements for manned space vehicles with extended on –orbit stay time", Acta Astronautica, Vol. 38, No. 2, pp. 115-123, 1996.
3. Dhillon, B. S., and Liu Y.,"Human error in maintenance: a review",Journal of Quality in Maintenance Engineering, Vol. 12, No. 1, pp. 21–36, 2006.
4. Duma, W. D., and Krieg K. J.,"DOD guide for achieving reliability, avaialbility and maintainbaility", Department of Defence, USA, 2005.
5. Drupsteen, L. and Hasle, P.,"Why do organizations not learn from incidents? Bottlenecks, causes and conditions for a failure to effectively learn",Accident Analysis and Prevention, Vol. 72, pp.351-358, 2014.
6. Dyadem, "Guidelines for failure mode and effect analysis for automotive, aerospace and general manufacturing industries", CRC Press, Boca Raton Florida, USA, 2003.
7. Ebling, C.E.,"An Introduction to Reliability and Maintainability Engineering", New Delhi, Tata McGraw Hill Publishing Company Limited, India, 1997.
8. Eti, M. C., Ogaji S.O.T., and Probert S.D.,"Integrating reliability, availability, maintainability and supportability with risk analysis for improved operation of the Afam thermal power-station" Applied Energy, Vol. 84, No. 2, pp.202-221, 2007.

9. Groote, P.De., "Maintenance performance analysis a practical approach", Journal of Quality in Maintenance Engineering, Vol., 1, No. 2, pp.4-24, 1995.
10. Horenbeek, A.V. and Pintelon L.,"Development of a maintenance performance measurement framework-using the analytic network (ANP) for maintenance indicator selection", Omega: The International Journal of Management Science, Vol.42, pp.33-46, 2014.
11. Jacopino, A., Groen F., and Mosleh A.,"Behavioural study of the general renewal process" IEEE Conference, RAMS, pp. 237-242, 2004.
12. Jostes, R.S., and Helms M.M.,"Total productive maintenance and its link to total quality management",Work Study, Vol. 43, No. 7, pp. 18-20, 1994.
13. Kelly, A., "Managing Maintenance Resources",Elsevier Limited, Jordan Hill, Oxford, UK, 2006.
14. Kijima, M., "Some results for repairable systems with general repair",Journal of Applied Probability, Vol. 26, No. 1, pp.89-102, 2013.
15. Kumar, U., Galar D., Parida A., and Stenstrom C.,"Maintenance performance metrics: a state-of-art review" Journal of Quality in Maintenance Engineering, Vol. 19, No. 3, pp.233-277, 2013.
16. Kutucuoglu, K.Y., Hamali J., Irani, Z., and Sharp, J.M.,"A framework for managing maintenance using performance measurement systems" International Journal of Operations and Production Management, Vol. 21, No. ½, pp. 173-194, 2001.
17. Latorella, K.A., and Prabhu, P.V., "A review of human error in aviation maintenance and inspection", International Journal of Industrial Ergonomics, Vol. 26, No. 2, pp.133-161, 2000.
18. Lofsten, H.,"Measuring maintenance performance – in search for a maintenance productivity index",International Journal of Production Economics, Vol. 63, pp. 47-58, 2000.
19. Marquez, A.C.,"The maintenance management framework, models and methods for complex systems maintenance",Springer Series in Reliability Engineering, Verlag London Limited, 2007.
20. Marquez A.C., and Gupta J.N.D., "Contemporary maintenance management: process, framework and supporting pillars", Omega The international Journal of Management Science, Vol. 34, pp. 313-326, 2006.
21. Matthews, C., "A practical guide to engineering failure investigation",Professional Engineering Publishing Limited, London and Bury St. Edmunds, UK, 1998.
22. Muchiri P., Pintelon L., Gelders L., and Martin, H.,"Development of maintenance function performance measurement framework and indicators",International Journal of production Economics, Vol. 131, pp.295-302, 2011.
23. Murthy D.N.P., Atrens A.and Eccleston A.,"Strategic maintenance management", Journal of Quality in Maintenance Engineering, Vol. 8, No. 4, pp. 287-305, 2002.
24. Neely A. ,"The performance measurement revolution: why now and what next?", International Journal of operations and Production Management, Vol. 19, No. 2, pp.205-228, 1999.
25. Neely A., M. Bourne, and M. Kennerley,"Performance measurement system design: developing and testing a process-based approach" International Journal of Operations and Production Management, Vol. 20, No. 10, pp. 1119-1145, 2000.
26. Parida A. and G. Chattopadhyay, "Development of a multi-criteria hierarchical framework for maintenance performance measurement (MPM)", Journal of Quality in Maintenance Engineering, Vol. 13, No. 3, pp. 241-258, 2007.
27. Parida A. and Kumar U.,"Maintenance performance measurement (MPM): issues and challenges",Journal of Quality in Maintenance Engineering, Vol. 12, No. 3, pp.239-251, 2006.
28. Pham H., and Wang H., "Imperfect Maintenance",European Journal of Operational Research, Vo. 94, No. 3, pp.425-438, 1996.
29. Pinjala S.K., Pintelon, L. and Vereecke, A.,"An empirical investigation on the relationship between business and maintenance strategies",International Journal of Production Economics, Vol. 104, pp. 214-229, 2006.
30. Pintelon L.M. and Gelders L.F.,"Maintenance management decision making", European Journal of Operational Research, Vol. 58, pp. 301-317, 1992.
31. Pintelon L.M. and Van Wassenhove L.N.,"A maintenance management toll",Omega The International Journal of Management Science, Vol. 18, No. 1, pp.59-70,1990.
32. Rai R. N. and Bolia N.,"Modified FMEA model with repair effectiveness factor using generalized renewal process" SRESA Journal of Life Cycle Reliability and Safety Engineering, Manuscript accepted for Publication, 2015.
33. Rai R. N. and Bolia, N.,"Select study of procurement process and availability improvement in military aviation", PhD Dissertation, Department of Mechanical Engineering, IIT Delhi, India, 2014.
34. Raouf A., "On evaluating maintenance performance",International Journal of Quality and Reliability Management, Vol. 10, No. 3, pp.33-36, 1993.
35. Raouf A. and Ben-Daya M.,"Total maintenance management: a systematic approach. Journal of Quality in Maintenance Engineering", Vol. 1, No. 1, pp. 6-14, 1995.
36. Sharma R. K. and Kumar S.,"Performance modeling in critical engineering systems using RAM analysis",Reliability Engineering and System Safety, Vol. 93, No. 6, pp. 913-919, 2008.
37. Sherwin D.J. and Jonsson P.,"TQM, maintenance and plant availability", Journal of Quality in Maintenance Engineering, Vol. 1, No. 1, pp. 15-19, 1995.
38. Simoes J.M., Gomes C.F., and Yasin M.M.,"A literature review of performance measurement: A conceptual framework and directions for future research",Journal of Quality in Maintenance Engineering, Vol. 17, No. 2, pp. 116-137, 2011.
39. Swanson L.,"An empirical study of the relationship between production technology and maintenance management",International Journal of Production Economics, Vol. 53, pp.191-207, 1997.
40. Swanson L.,"Linking maintenance strategies to performance", International Journal of Production Economics, Vol. 70, pp. 237-244, 2001.
41. Tanwar M., Rai R.N., and Bolia N.,"Imperfect repair using Kijima type generalized renewal process", Reliability Engineering and System Safety, Vol. 124, pp.24-31, 2014.
42. Tinga T.,"Principles of Loads and Failure Mechanisms: Applications in Maintenance, Reliability and Design",Springer Series in Reliability Engineering, Springer-Verlag, London, UK, 2013.

43. Tsang A.H.C.,"A strategic approach to managing maintenance performance", Journal of Quality in Maintenance Engineering, Vol. 4, No. 2, pp. 87-94, 1998.
44. A.H.C. Tsang,"Measuring maintenance performance: a holistic approach", International Journal of Operations and Production Management, Vol. 19, No. 7, pp. 691-715, 1999.
45. Visser J.K. and Pretorius M.W.,"The development of a performance measurement system for maintenance", SA Journal of Industrial Engineering,Vol.14, No. 1, pp.83-97, 2003.
46. Waeyenbergh G. and Pintelon, L.,"CIBOCOF: A framework for industrial maintenance concept development", International Journal of Production Economics, Vol. 121, pp.633-640, 2009.
47. Yanez M., Joglar F., and Modarres, M., "Generalized renewal process for analysis of repairable systems with limited failure experience",Reliability Engineering and System Safety, Vol. 77, pp.167-180, 2002.
48. Yu Q., Guo H., and Liao H.,"An analytical approach to failure prediction for systems subject to general repairs", IEEE Transactions on Reliability, Vol. 62, No. 3, pp.714-721, 2013.
49. Zerwick A.Y., "A focused approach to reliability, availability and maintainability for critical pressure vessels",International Journal of Pressure Vessels and Piping, Vol.66, No. 1-3, pp. 155-160, 1996.
50. Zhu G., Gelders L., and Pintelon L., "Object/objective oriented maintenance management", Journal of Quality in Maintenance Engineering, Vol. 8, No. 4, pp.306-318, 2002.

Life Cycle Reliability and Safety Engineering
Vol.5 Issue 1 (2016) 29-42

Loss of life of Induction Motors under various operating anomalies

Tarun Chugh[1], P.V. Varde[2]
[1]*Nuclear Power Corporation of India Limited, Anushaktinagar, Mumbai, India*
[2]*Bhabha Atomic Research Centre, Trombay, Mumbai, India*
Email: tchugh@npcil.co.in

Abstract

Reliability studies conducted to study the various failure modes of an induction motor shows that one of the failure modes i.e. winding failure is quite prevalent and accounts for high percentage of failures of motors. Thus, there is a pivotal need to understand the theory of winding failure and know how it can be prognosticated based on the input parameters, current operating environment and maintenance history of a motor. This paper defines loss of motor life as the loss of stator winding insulation life due to thermal and environmental stresses. From the thermal point of view, the stator winding insulation is the weakest part of a squirrel cage induction motor, and equations are developed to estimate the insulation life and hence the motor life. In this regard, an integrated model consisting of an electrical model, thermal model and insulation ageing model is developed to evaluate the effect of various anomalies/stressors e.g. overvoltage and voltage unbalance on the life of a motor. This model is used to quantify the loss of life of a 2.3 kW, 415 V induction motor. The electrical model is developed by conducting Open Circuit and Blocked Rotor Test on the motor and thereby deriving its equivalent circuit. Using the model, the stator winding losses are calculated and given as an input to the thermal model to find the temperature rise in the stator winding. The steady state temperature of the stator winding is given as an input to the insulation aging model which predicts the loss of life. This work presents a simple technique for calculating thermal parameters based on motor testing rather than from motor design data. The insulation ageing model is developed based on Eyring Equation considering temperature and humidity as stressors.

Keywords: Induction Motors, Winding Insulation, remaining life, Eyring Equation

1. Introduction

Induction Motors are the workhorses of the industry. Such motors are robust machines used not only for general purposes, but also in hazardous locations and severe environment. General purpose applications of induction motors include pumps, conveyors, machine tools, centrifugal machines, presses, elevators, and packaging equipment. Additionally, induction motors are highly reliable, require low maintenance, and have relatively high efficiency. Moreover, the wide range of power of induction motors, which is from hundreds of watts to megawatts, satisfies the production needs of most industrial processes. Although induction motors are constructed, tested, and qualified to rigorous standards, failures of electric motors in plants continue to occur. Operating anomalies, failures of other equipment, and other unforeseen circumstances can all contribute to aging in motors. Healthiness of the machines contributes to the production, down time reduction, reliability and revenues.

Monitoring of the healthiness of the machines, therefore, is very important and essential. The ability to accurately predict changes in properties/parameters of electrical machines is of critical importance in optimizing the maintenance schedule of the plant. Thus, there is a continuous need to device test methods or to find more searching and sensitive parameters to predict the machine health. In view of this, it becomes quite important for a maintenance engineer to be able to predict the health of motor leading to appropriate usage of the machine(s), reduction in downtime, enhanced operational reliability & safety and revenues. Thus, the maintenance action can be optimized by diagnostics and prognostics methods which form a part of Condition Based Maintenance (CBM).

The stressors that affect electric motors are: Heat, Chemicals, Pressure, Steam, Radiation, Mechanical Cycling/Rubbing, Humidity/Water Spray, Electromagnetic Cycling, Vibration/Seismic, and Foreign Object Ingestion.

These stressors act independently and/or synergistically to cause failures in the major subcomponents of electric motors, such as the stator windings, electrical terminations, bearings, and rotor cage. All of the stressors listed above contribute to the gradual or catastrophic degradation of the insulation system. Mechanical and electromagnetic cycling, ingestion of foreign objects, and vibration-related stressors act upon the mechanical integrity of the machine. They can cause bearing and lubrication system problems, rotor breakage, mounting/enclosure failures, and failures of the shaft/couplings.

Recent studies regarding the operating experience of electric motors and the effects of aging on electrical equipment have indicated that many electric motor failures can be attributed to the aging and degradation of insulating materials and bearings caused by high temperature, vibration, moisture and other stressors [1, 2].

The stator winding system plays an important role in induction motors. The stator winding is the weakest part of a squirrel cage induction motor from the thermal point of view. Thus, there is a pivotal need to understand the theory of winding failure and know how a winding failure can be prognosticated based on the input parameters, current operating environment and maintenance history of a motor. In this regard, an integrated model consisting of an electrical model, thermal model and insulation ageing model is developed to evaluate the effect of various anomalies/stressors on the life of motor. This model is used to quantify the loss of life of a 2.3 kW, 415 V induction motor.

2. Stresses on the insulation system of induction motor

Any rotating machine e.g. induction motor has two types of insulation; groundwall insulation and conductor insulation. Groundwall insulation separate those components that may not be in galvanic contact with each other. E.g. Groundwall insulation galvanically separates coil from iron core of machine. Conductor insulation separates wires and turns of a coil.

Insulation systems are rated by standard NEMA (National Electrical Manufacturers Association) classifications according to maximum allowable operating temperatures as shown in Table 1 [3].

The main cause for insulation failures can be divided into four groups: thermal, electrical, mechanical and environmental-stress [4]

2.1. Thermal Stress:

One of the thermal stresses the insulation is subject to is the thermal aging process. An increase in temperature accelerates the aging process and thus reduces the lifetime of the insulation significantly. As a rule of thumb, 10 degrees increase in temperature decreases the insulation life by 50% [4]. Under normal operating conditions the aging process itself does not cause a failure, but makes the insulation more vulnerable to other stresses, which then produce the actual failure. In order to ensure a longer lifetime and reduce the influence of the aging process one can either work at low operating temperatures or use an insulation of higher quality, i.e. use a higher insulation class.

Another thermal stress that has a negative effect on the insulation lifetime is thermal overloading, which occurs due to voltage variations, unbalanced phase voltages, cycling, overloading, obstructed ventilation or ambient temperature. For example, even a small increase in the voltage unbalance has an enormous effect on the winding temperature. As a rule of thumb, the temperature in the phase with the highest current will increase by 25% for a voltage unbalance of 3.5% per phase [4].

Voltage Unbalance: The greatest effect of voltage unbalance is on three-phase induction motors. Three phase induction motors are one of the most common loads on the network and are found in large numbers especially in industrial environments.

Table 1: NEMA Classification of Insulation System

Temperature Tolerance Class	Maximum Operation Temperature Allowed		Allowable Temperature Rise at full load (1.0 service factor)	Allowable Temperature Rise (1.15 service factor)
	°C	°F	°C	°C
A	105	221	60	70
B	130	266	80	90
F	155	311	105	115
H	180	356	125	-

Negative phase sequence in induction motors is caused due to unbalanced voltages in the supply voltage applied on the stator terminals or unbalanced windings.

Negative phase sequence components create a rotating magnetic field in the stator which moves in the opposite direction. This causes a decrease in the torque developed by the motor. The motor will thus have to draw a higher current for the same mechanical load

It should be ensured that the flow of air through the motor is not obstructed since the heat cannot be dissipated otherwise and the winding temperature will increase. If this is not possible however, this should be taken into account by upgrading the insulation system or restricting the winding temperature.

2.2 Electrical Stress:

There are different reasons why electrical stresses lead to failure of the stator insulation. These can usually be broken down into problems with the dielectric material, the phenomena of tracking and corona and the transient voltages that a machine is exposed to. The type of dielectric material that is used for phase-to ground, phase-to-phase and turn-to-turn insulation as well as the voltage stresses applied to the insulating materials, influence the lifetime of the insulation significantly. Thus, the materials for the insulation have to be chosen adequately in order to assure flawless operation and desired design life.

The negative influence of transient voltage conditions on the winding life has been observed in recent years. These transients, that either cause deterioration of the winding or even turn-to-turn or turn-to-ground failures, can be caused by line-to-line, line-to-ground or multiphase line-to-ground faults in the supply, repetitive restriking, current limiting fuses, rapid bus transfer, opening and closing of the circuit breakers, capacitor switching (power factor improvement), insulation failure in the power system or lightning strike. Variable frequency drives are subject to permanent voltage transients. Especially during the starting and stopping process high voltage transients can occur.

2.3 Mechanical Stress:

The main causes for insulation failure due to mechanical stresses are coil movement and strikes from the rotor. The force on the winding coils is proportional to the square of the motor current and reaches its maximum value during the startup of the motor. This force causes the coils to move and vibrate. The movement of the coils again can cause severe damage to the coil insulation or the conductor.

There are different reasons that will cause the rotor to strike the stator. The most common are bearing failures, shaft deflection and rotor-to-stator misalignment. Sometimes the contact is only made during the start but it can also happen that there will be a contact made at full speed of the motor. Both contacts can result in a grounded coil. There are other mechanical stresses, which the windings are exposed to, like loose rotor balancing weights, loose rotor fan blades, loose nuts or bolts striking the motor or foreign particles that enter the motor.

2.4 Environmental Stress:

Environmental stress can also be called contamination. The presence of foreign material can lead to reduction in the heat dissipation, premature bearing failure or even the breakdown of the insulation system by causing shorts. If possible the motor should be kept clean and dry internally as well as externally, to avoid the influence of moisture, chemicals and foreign particles on the insulation condition [4].

3. Integrated approach to remaining life estimation

3.1 General

In order to estimate motor life, an integrated approach is used where electrical, thermal and insulation ageing model are developed. This is shown in Figure 1.

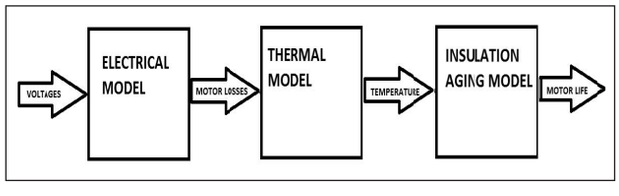

Figure 1: Motor Life Prediction Flowchart

From the flowchart it can be seen that the first step to determine the remaining life is development of an electrical model using motor design data and use it to calculate the losses. The electrical model is obtained by conducting Open Circuit and Blocked Rotor Tests on an induction motor which is used to evacuate the winding losses. The losses that eventually cause the heating of a winding of induction motor are an input to the thermal model which is based on a single time constant thermal model. The temperature rise depends on the thermal resistance, thermal capacitance, ambient temperature and losses. The thermal model

gives the temperature which is the input to the thermal ageing model. The thermal ageing model is based on Eyring Equation using constants for a typical class B insulation system. This model which assumes that insulation degradation is a function of temperature and humidity, gives the remaining life of the insulation as the output.

3.2 Electrical Model of Induction Motor

The electrical model is used to simulate the motor's electrical performance characteristics. The per phase electrical model of the induction motor, with rotor referred with respect to the stator can be represented as shown in Figure 2.

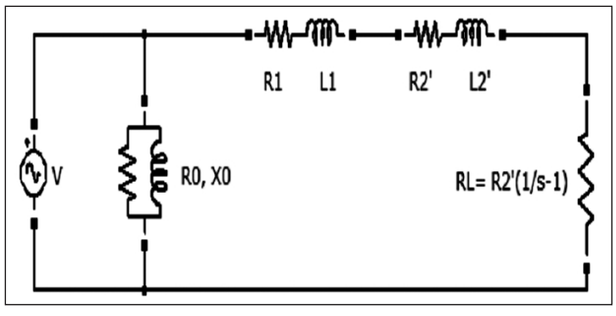

Figure 2: Equivalent Circuit (Per Phase) of induction motor

Where the various parameters are explained below in Table 2.

Table 2 Equivalent circuit parameters of induction motor

Parameter Symbol	Parameter
V	Voltage (Phase to ground)
I1	Stator Current
I0	Magnetising current
I1′	Total current
R0	No Load resistance
X0	No Load leakage reactance
R1	Stator resistance (Per phase)
X1	Stator reactance (Per phase)
R2′	Rotor resistance (referred to stator)
X2′	Rotor reactance (referred to stator)
RL	Load resistance
S	Slip

3.3 Determination of equivalent circuit of motor using No-Load and Blocked Rotor Test

3.3.1 No-Load Test

The no load test on an induction motor gives information with respect to exciting current and no-load losses. The test is performed at rated frequency and with balanced polyphase voltages applied to the stator terminals. Readings are taken at the rated voltage, after the motor runs long enough for the bearings to be properly lubricated.

The behaviour of the machine may be judged from the equivalent circuit of Fig. 3 and the parameters are shown in Table 3. The current drawn by the machine causes a stator-impedance drop and the balance voltage is applied across the magnetizing branch. However, since the magnetizing branch impedance is large, the current drawn is small and hence the stator impedance drop is small compared to the applied voltage (rated value). This drop and the power dissipated in the stator resistance are therefore neglected and the total power drawn is assumed to be consumed entirely as core loss. The current drawn is at low power factor. This test enables us to compute the resistance and inductance of the magnetizing branch in the following manner as shown from equations (1) - (6) [5].

Table 3 No-load Equivalent circuit parameters of induction motor

S.No.	Parameter	Symbol
1	Voltage (No-Load)	
2	Current (No-Load)	
3	Power Factor (No-Load)	
4	Power (No-Load)	
5	Stator Winding Resistance	
6	Magnetizing Current	
7	No Load resistance	
8	No Load leakage reactance	

$$\text{No load per phase current} = \frac{I_{NL}}{\sqrt{3}}$$

$$P_{stator\_winding=} \; 3 * (\frac{I_{NL}}{\sqrt{3}})^2 * R_{Stator} \quad (1)$$

$$P_{NL} = 3 * V_{NL} * \frac{I_{NL}}{\sqrt{3}} * P.F_{NL} \quad (2)$$

$$R0 = \frac{\sqrt{3} * V_{NL}}{(I_{NL} * P.F_{NL})} \quad (3)$$

$$Im = \sqrt{((I_{NL})^2 - (I_{NL} * P.F_{NL})^2)} \quad (4)$$

$$X0 = \frac{\sqrt{3} * V_{NL}}{(Im)} \quad (5)$$

3.3.2 Blocked Rotor Test (6)

Like the short-circuit test on a transformer, the Blocked-Rotor test on an induction motor gives information with respect to the leakage impedances. The rotor is blocked so that it cannot rotate (hence the slip is equal to unity), and balanced poly-phase voltages are applied to the stator terminals.

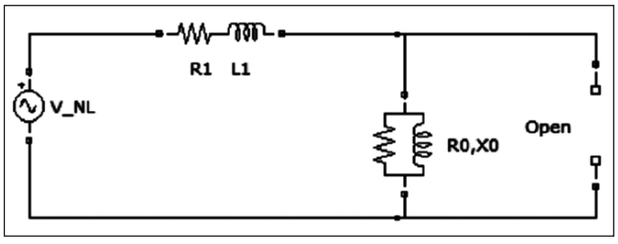

Figure 4: Equivalent Circuit at Blocked-Rotor

The equivalent circuit for blocked-rotor conditions is identical to that of a short circuited transformer as shown in Figure 4. An induction motor is more complicated than a transformer, however, because its leakage impedance may be affected by magnetic saturation of the leakage-flux paths and by rotor frequency. The guiding principle is that the blocked-rotor test should be performed under conditions for which the current and rotor frequency are approximately the same as those in the machine at the operating condition for which the performance is later to be calculated.

The total leakage reactance at normal frequency can be obtained from this test by considering the reactance to be proportional to frequency. The effects of frequency often are negligible for normal motors of less than 25-hp rating, and the blocked impedance can then be measured directly at normal frequency. The importance of maintaining test currents near their rated value stems from the fact that these leakage reactances are significantly affected by saturation. Based upon blocked-rotor measurements, the blocked-rotor resistance can be found from the blocked-rotor voltage and current as shown below. Similarly, the blocked rotor reactance can be found. Once these parameters have been determined as shown in equations (7)-(14), the equivalent circuit parameters given in Table 4 can be determined.

Table: 4 - Blocked rotor equivalent circuit parameters of induction motor

Sr. No.	Parameter	Symbol
1	Voltage (Blocked Rotor)	
2	Current (Blocked Rotor)	
3	Power Factor (Blocked Rotor)	
4	Power (Blocked Rotor)	
5	Equivalent Impedance	
6	Equivalent reactance	
7	Equivalent resistance	

$$\text{Short Circuit Stator phase current} = \frac{I_{BR}}{\sqrt{3}} \quad (7)$$

$$Z01 = \frac{\sqrt{3} * V_{BR}}{I_{BR}} \quad (8)$$

$$R01 = \frac{P_{BR}}{{I_{BR}}^2} \quad (9)$$

$$X01 = \sqrt{(Z01)^2 - (R01)^2} \quad (10)$$

$$R01 = R1 + R2' \quad (11)$$

$$X01 = X1 + X2' \quad (12)$$

$$X1 = 0.5 * X01 \quad (13)$$

$$X2' = 05 * X01 \quad (14)$$

Thus the induction motor parameters can be found using No-Load and Blocked rotor test using equations (1)-(14).

3.4 Determination of winding copper loss

The stator winding losses are calculated using the data given in Table 5 and equations (15)-(22) by finding the equivalent load resistance which is a function of the slip.

Table 5. Parameters of induction motor

S.No.	Parameter	Symbol
1	Rotor Speed	
2	Synchronous Speed	
3	Slip	
4	Load resistance	
5	Shunt Impedance	
6	Effective Impedance	

$$\text{Speed (Nr)} = \frac{\text{Nr RPM}}{\text{Syncoronous Speed (Ns)}}$$

$$\text{Slip (s)} = \frac{Ns - Nr}{Ns} \quad (15)$$

$$RL' = R2'\left(\frac{1}{s} - 1\right) \quad (16)$$

$$Z_{sh} = R0||X0 \quad (17)$$

$$Z_{eff} = (R1 + R2' + RL') + j(X1 + X2') \quad (18)$$

$$I1' = \frac{V}{Z_{eff}} \quad (19)$$

$$I0' = \frac{V}{Z_{sh}} \quad (20)$$

$$I = I0' + I1' \quad (21)$$

$$P_{winding} = 3 * I^2 * R_{stator} \quad (22)$$

3.5 Effect of Overvoltage

When the motor is subjected to overvoltage, there is an increased current flowing through the stator windings. This increased current leads to higher winding temperature, which causes accelerated degradation of the motor insulation. The level of degradation or loss of life of the motor is quantified using Arrhenius/ Eyring equation.

3.6 Effect of Voltage Unbalance

An excessive level of voltage unbalance can have serious impacts on mains connected induction motors. The level of current unbalance that is present is several times the level of voltage unbalance. Such an unbalance in the line currents can lead to excessive losses in the stator and rotor that may cause protection systems to operate causing loss of production. Although induction motors are designed to tolerate a small level of unbalance they have to be de-rated if the unbalance is excessive. If operated at the nameplate rated capacity without de-rating the useful life of such induction motors can become quite short. If an induction motor is oversized to a given application then some level of protection is built into its operation although the motor does not operate at the best efficiency and power factor [6].

Causes of voltage unbalance include unequal impedances of three-phase transmission and distribution system lines, large and/or unequal distribution of single-phase loads, phase to phase loads and unbalanced three-phase loads. When a balanced three-phase load is connected to an unbalanced supply system the currents drawn by the load also become unbalanced.

NEMA (National Electrical Manufacturers Association of USA) standard definition that is given by equation (23).

$$\text{Voltage unbalance} = \frac{\text{Maximum deviation from mean of}(V_{ab}, V_{bc}, V_{ca})}{\text{Mean of}(V_{ab}, V_{bc}, V_{ca})} \quad (23)$$

Negative phase sequence components create a rotating magnetic field in the stator which moves in the opposite direction. This causes a decrease in the torque developed by the motor. The motor will thus have to draw a higher current.

The rotating magnetic field which rotates in the opposite direction induces voltages in the rotor. These voltages have a frequency that is double the system frequency. Since the frequency of this rotor voltage is higher, it flows on the surface of the rotor due to the skin effect and causes surface heating which can lead to motor damage.

If the motor is fully loaded some stator phase windings and the rotor will carry more current than that is permitted thus causing extra motor losses. This will lead to a reduction in motor efficiency while reducing the insulation life caused by overheating.

In addition to reduced efficiency, overheating and loss of insulation life, induction motors operating with unbalance will be noisy in their operation caused by torque and speed pulsations. Obviously in such situations the effective torque and speed will be less than normal.

To study the effect of unbalance voltage on the life of winding, sequence component theory is used to derive the positive and negative sequence component of voltages as shown in equation (24).

$$\begin{bmatrix} V1 \\ V2 \\ V0 \end{bmatrix} = \frac{1}{3}\begin{bmatrix} 1 & \alpha & \alpha^2 \\ 1 & \alpha^2 & \alpha \\ 1 & 1 & 1 \end{bmatrix}\begin{bmatrix} Vab \\ Vbc \\ Vca \end{bmatrix} \quad (24)$$

Where, $\alpha = 1\angle 120$ degree

V1, V2 and V0 are the positive, negative and zero sequence components of the line voltages Vab, Vbc and Vca. The positive sequence voltage V1 is used to find the positive sequence current I1.

Using the positive sequence component of voltage, the positive sequence circuit as shown in Figure 5 is used to analyse the motor behavior under voltage unbalance condition.

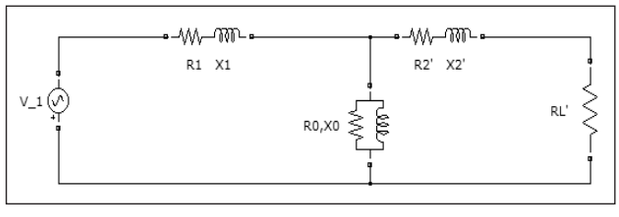

Figure 5: Positive Sequence Equivalent Circuit

The negative sequence current (I2) is found as shown in equation (25):

$$I^2 = I1^2 + I2^2 \quad (25)$$

Also, the ratio of positive sequence impedance to negative sequence impedance equivalent to ratio of starting current to full load current. Thus the negative sequence current can be calculated by multiplying the

negative sequence voltage with the ratio of starting to full load current.

The stator winding loss is found as shown in equation (26):

$$P_{winding} = 3 * I^2 * R_{stator} \quad (26)$$

4. Thermal Model of an Induction Motor

In the second stage, the output of the electrical models i.e. the I^2R losses is used to estimate the winding temperature of the stator. The thermal model of an induction motor is based on single thermal capacitance and single thermal resistance i.e. with single thermal time constant. The thermal capacitance and thermal resistance are normally predetermined by a set of parameters for a given class of motors, classified by their full load current (FLC), service factor (SF) and trip class (TC). Otherwise, these constants can be determined experimentally.

Thermal models with a single thermal capacitor and single thermal resistor are derived from the heat transfer of a uniform object, as shown in Figure 6 [7].

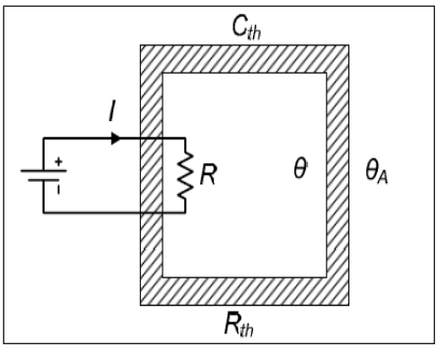

Figure 6: Heat Transfer model with single thermal time constant

The quantities θ and θ_A, in ^{0}C, are temperatures of the uniform object and its ambient, respectively. The power input into this uniform object is determined by the power losses from the current, I (Unit: A), on the resistor, R (Unit: Ohms). Heat is dissipated through the boundary of the uniform object (the shaded region in Figure 6) to the ambient. The thermal resistance, Rth, in ^{0}C/W, models this heat transfer. The thermal capacitance, Cth, in J/^{0}C, is defined to be the energy needed to elevate temperature by one degree Celsius for the object. It represents the total thermal capacity of the object.

The difference between the input power and the output power is used to elevate the temperature of the uniform object.

$$Pin - Pout = Cth * \frac{d(\theta - \theta_A)}{dt} \quad (27)$$

The input power is the heat, I^2R, generated by the current in the resistor. The output power is the heat transfer,, across the boundry of the object to its ambient. Therefore, the above equation can be written as shown in equation (28)

$$I^2R - \frac{\theta - \theta_A}{Rth} = Cth * \frac{d(\theta - \theta_A)}{dt} \quad (28)$$

Solving the above equation as a first order differential equation, a closed form solution is obtained in equation (29).

$$\theta(t) = I^2R.Rth\left(1 - e^{-\frac{t}{\tau th}}\right) + \theta_A \quad (29)$$

which is the thermal time constant of the motor.

If the constant current, I, flows through this uniform object for a sufficiently long time, i.e. for $t \to \infty$, the final temperature is

$$\theta(\infty) = I^2R.Rth + \theta_A \quad (30)$$

For a specific motor, it is designed to work under some permissible temperature, θ_{max}, determined by the stator winding insulation material. This maximum temperature determines the maximum permissible current through the stator winding as shown in equation (31),

$$Imax = \sqrt{(\theta_{max} - \theta_A)/R.Rth} \quad (31)$$

For a motor, if the stator current exceeds a predetermined value for a certain time, the stator winding temperature will rise above its maximum permissible value.

Thus the stator winding temperature as a function of time and current can be written as in equation (32) :

$$(\theta_{max} - \theta_A)(I/I\_max)^2\left(1 - e^{-\frac{t}{\tau th}}\right) + \theta_A \quad (32)$$

For a typical induction motor, the temperature rise in the stator windings as a function of time is shown in Figure 7.

5. Insulation Ageing Model

5.1 General

With time, the insulation becomes brittle and shrinks, leading to cracks. The insulation at the point

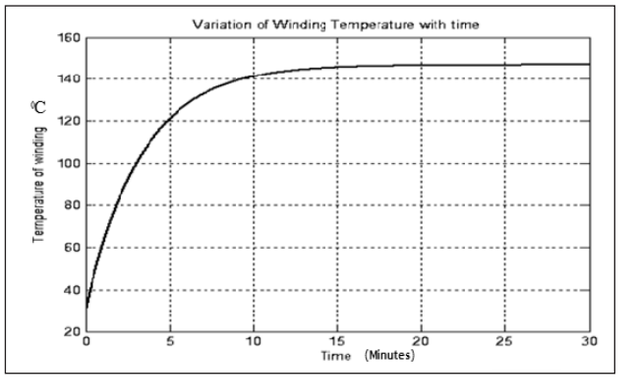

Figure 7: Typical variation of stator winding temperature with time with ambient temperature 30 ^{0}C

of cracks weakens gradually as surrounding pollutants find their way through these cracks. The weakening of insulation with time is called 'ageing'.

The life of the insulation will also be affected by an excessive operating temperature. Ageing occurs when a machine is occasionally over-loaded. Sometimes the size of the machine may be only marginal when it was initially chosen and with the passage of time, it may be required to perform duties that are too arduous. Every time the machine over-heats, the insulation deteriorates, and this is called thermal ageing of insulation.The insulating system is one of the main parts of electrical rotary machine. High operating and reliability demands require the proper technological steps to manufacture the insulating system. Much effort has been invested over several decades in studying the aging characteristics of the various electrical insulating system designs and insulating materials employed in high-voltage equipments. These studies aim mainly to allow reasonable estimates of the service life expectancies of such equipment and to assess their reliability in operating conditions after a given number of years in service. The aging of a polymeric material, or of any other material for that matter, inherently involves the alterations of the material's physical and/or chemical structure which is expected to be related to the changes in the physical and chemical properties of the material. When the aging of a dielectric material is evoked, it usually implies that the alterations in the properties of the material are detrimental to its service operation and service reliability. When these properties have deteriorated to the point where the material can no longer operate safely under normal stress conditions, it implies that it has reached the end of its useful life. The causes of aging are yet to be fully understood, but obviously, the degree of aging strongly depends on the nature of the involved material and on the nature and duration of the applied stresses. Indeed, aging can be induced by a combination of the various stresses (electrical, mechanical, thermal or environmental) to which the insulation system is subjected. The simultaneous application of these stresses leads to the interaction of aging mechanisms [8,9,10].

5.2 Eyring Model

Chemical reactions in progress between water ions and insulation (hydrolysis) may lead to insulation destruction. Insulation mechanical properties can disrupt with moisture. Electrical properties with moisture absorption changing significantly (material dielectric strength significantly change, dielectric losses increase, electric stress structure redistribution). This leads to sparkover, to insulation surface breach due to partial discharges followed by erosion of insulation surface. Synergistic effects may occur between an electric field and humidity, which can lead on some polymers to creating water trees. Dynamics of condensation, capillarity and absorption and resulting material changes depends on exposure to moisture mode (steam or liquid).

Therefore, it has been seen that besides temperature, another factor that causes accelerated degradation of motor winding insulation is humidity. Thus, there is a need to redefine the insulation ageing model taking into consideration the effect of humidity also. This can be done using Eyring's Model which is an extended version of Arrhenius Model. The Eyring's Model is explained below and represented as in equation (33)

The key to this model formulation was thorough understanding of model parameters based on two independently changing degradation factors – humidity and temperature.

$$\ln\left(\frac{tr}{ti}\right) = \left(\frac{Ti}{Tr}\right)\left(\frac{Ea}{k} * \left(\frac{1}{Tr} - \frac{1}{Ti}\right)\right)\left(\frac{Eb}{k} * \left(\frac{1}{RHr} - \frac{1}{RHi}\right)\right) \quad (33)$$

tr time at temperature Tr

ti time at temperature Ti

RHr is relative humidity at temperature Tr

RHi is relative humidity at temperature Ti

(Activation Energy for temperature)= 1.05 eV for Class F insulation

(Activation Energy for humidity)= Unknown

K =0.8617* 10−4 eV/K

5.3 Effect of Frequent Start/Stops

Repeated motor starts also contribute to reduction in life due to increased temperatures since all losses in an electric motor are converted into heat. Part of this heat energy is dissipated by the motor through the mechanisms of thermal radiation, conduction and convection, while the remainder of this energy causes the temperature of the motor to rise. When the heat absorption by the motor becomes zero, or in different words, when the rate of heat dissipated becomes equal to the rate of heat generated by the motor, steady-state temperature is reached. This temperature in a properly designed motor represents the temperature rating of its insulation system (temperature rise in the insulation plus the hottest spot allowance plus the temperature of the ambient).

It remains then to determine what magnitude of heating may be expected on motor stator windings. Calculations of this are approximate in that all the heat generated during the interval of acceleration is assumed to be absorbed and that the conductor cross-section follows an average practice, namely that 500 circular mils per ampere (0.253 sq. inch/ampere) (at full load) is used.

With these assumptions, the temperature rise in the stator windings can be calculated, using the following expression in (34):

$$T = 2.3 * \frac{10^4}{D^2} \qquad (34)$$

where T is the temperature rise, OC, D is the circular in mils per ampere (5.061 x 10^{-4} mm^2/ ampere). Assuming, for example, that a motor-driven equipment requires 30 s to reach operating speed, that the current during this period is 5 x the full-load current (on the average), and that the motor stator conductors have a cross-section of 500 circular mils per ampere (0.253 mm^2/ampere) at normal full load, the per-ampere area is effectively reduced to 100 circular mils. Thus, the total temperature rise at the end of one start is, by above equation, T = 2.3 x $104/100^2$ x 30 = 69°C.

If one assumes that this motor is started right after it has been shut off, then this temperature rise of 69°C can be added to the operating temperature. Thus, the windings experience a temperature 69°C above its classification temperature rating.

If two additional assumptions are made, namely that (1) the insulation ageing curve has a 10°C slope, or that for every 10°C rise the rate of insulation deterioration doubles, and that (2) the rounded-off temperature rise is 70^0C, then during the acceleration period the rate of deterioration will be increased by a factor of $2^{70/100}$, or will be 128 x that for the normal temperature. At this rate of deterioration, the 30 s accelerating period will be equivalent to 30 x 128 or 3840 s - about one hour. Each motor start, therefore, will reduce the calculated life by one hour. This is a conservative estimate which can be more accurately determined by calculating the changes in life expectancies incrementally for each second of temperature rise [8].

6. System Configuration

6.1 General

The integrated approach elucidated above is used to predict the remaining life of a 2.3 kW, 415 V, 3 Phase induction motor under various operating anomalies e.g. Over-voltage and voltage unbalance. The experimental setup is shown in Figure 9. Supply is fed though a 3 phase auto-transformer.

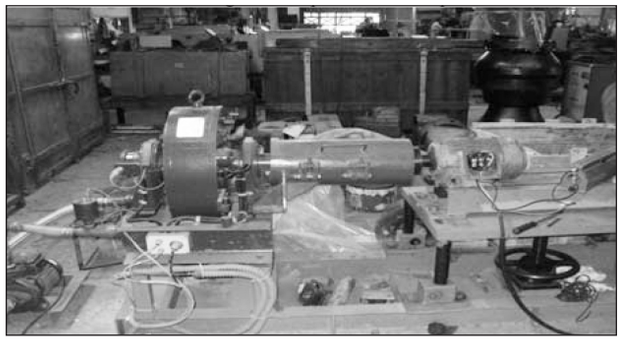

Figure 9: Experimental Setup

The load used is an Eddy Current Dynamometer which works as the load.

6.2 Determination of equivalent circuit of motor using No-Load and Blocked Rotor Test

Stator Winding Resistance = 3.5 Ohms

Insulation Resistance= 4 M –ohms

6.2.1 No-Load Test Results

Table 6 shows the No load Test Results and circuit parameters as found based on equation (35)- (41).

Table 6 : No-load Test Results

S.No.	Parameter	Symbol	Value
1	Voltage	V_{NL}	415 V
2	Current	I_{NL}	3.1 A
3	Power Factor	$P.F._{NL}$	0.134
4	Power	P_{NL}	296.95 W
5	Stator Winding Resistance	R_Stator	3.5 Ohms
6	Magnetising Current	Im	3.02 A
7	No Load resistance	R0	1730 ohms
8	No Load leakage reactance	X0	233.98 ohms

$$\text{No load per phase current} = \frac{I_{NL}}{\sqrt{3}} = 1.78 \text{ A} \quad (35)$$

$$P_{stator\_winding=} 3 * (1.78)^2 * 3.5 = 33.26 \text{ W} \quad (36)$$

$$P_{Friction} + P_{Windage} + P_{NL} = 750 - 33.26 = 716.73 \text{ W} \quad (37)$$

$$P_{NL} = 3 * 415 * 1.78 * 0.134 = 296.95 \text{ W} \quad (38)$$

$$R0 = \frac{\sqrt{3} * V_{NL}}{(I_{NL} * P.F_{NL})} = 1730.38 \text{ Ohms} \quad (39)$$

$$Im = \sqrt{((I_{NL})^2 - (I_{NL} * P.F_{NL})^2)} = 3.02 \text{ A} \quad (40)$$

$$X0 = \frac{\sqrt{3} * V_{NL}}{(Im)} = 233.98 \text{ ohms} \quad (41)$$

6.2.2 Blocked Rotor Test Results

Table 7 shows the Blocked Rotor Test Results and circuit parameters as found based on equation (42)-(45).

Table 7 : Blocked-Rotor Test Results

S.No.	Parameter	Symbol	Value
1	Voltage	V_{BR}	50 V
2	Current	I_{BR}	4.4 A
3	Power Factor	$P.F._B$	0.4
4	Power	P_{BR}	150 W
5	Equivalent Impedance	Z01	19.68 Ohms
6	Equivalent reactance	X01	18.08 Ohms
7	Equivalent resistance	R01	7.75 Ohms

$$\text{Short Circuit Stator phase current} = \frac{I_{BR}}{\sqrt{3}} = 2.54 \text{ A} \quad (42)$$

$$Z01 = \frac{\sqrt{3} * V_{BR}}{I_{BR}} = 19.68 \text{ Ohms} \quad (43)$$

$$R01 = P_{BR}/I_{BR}{}^2 = 7.75 \text{ Ohms} \quad (44)$$

$$X01 = \sqrt{(Z01)^2 - (R01)^2} = 18.089 \text{ Ohms} \quad (45)$$

Figure 9 shows the equivalent circuit of an induction motor as derived from No-Load and blocked rotor tests. The circuit parameters are derived from equations (46)-(49) and are shown in Table 8.

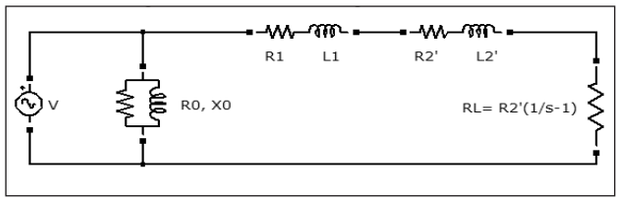

Figure 9: Induction motor equivalent circuit

Table 8 : Equivalent circuit parameters of induction motor

Parameters	Value
R0	1730.38 Ohms
X0	233.98 Ohms
R1	3.5 Ohms
X0	4.25 Ohms
R1	9.04 Ohms
$R2^{'}$	9.04 Ohms

6.3 Determination of winding copper loss

Stator winding loss is calculated based on the parameters shown in Table 9 and calculated as per equations (50)-(54).The stator winding copper losses are a function of the load (slip) and effective impedance seen with respect to primary. The load resistance is calculated which varies with the slip and so does the effective impedance. The shunt impedance, however, is independent of the slip.

Table 9: Parameters of induction motor

Parameter	Symbol	Value
Rated Speed	Nr	1430 RPM
Synchronous Speed	Ns	1500 RPM
Slip	s	0.046
Load Resistance	$RL^{'}$	88.14 Ohms
Shunt Impedance	Z_{sh}	Ohms
Effective Impedance	Z_{eff}	Ohms

$$\text{Speed (Nr)} = \quad 1430 \text{ RPM}$$
$$\text{Synchronous Speed (Ns)} = \quad 1500 \text{ RPM}$$

$$\text{Slip (s)} = \frac{Ns - Nr}{Ns} = 0.046 \tag{50}$$

$$RL' = R2'\left(\frac{1}{s} - 1\right) = 88.14 \text{ Ohms} \tag{51}$$

$$Z_{sh} = R0||X0 = 31.07 + j229.78 \tag{52}$$

$$Z_{eff} = \quad (R1 + R2' + RL') + j(X1 + X2')$$
$$= 95.89 + j18.08 \tag{53}$$

$$I = 4.8 \text{ A}$$
$$P_{winding} = 3 * I^2 * R_{stator} = 80.73 \text{ W} \tag{54}$$

6.4 Temperature Measurement

The motor was coupled with the load and run at full load. Temperature of the stator winding was found and the following observations were made as shown in Table 10 and Figure 10.

Table 10: Induction Motor- Temperature measured at various intervals

Time (Minutes)	Temperature (^{0}C)
0	30
5	39
10	44.7
15	47.2
20	48.8
25	49.5
30	49.7
40	50
50	50.1
60	50.1

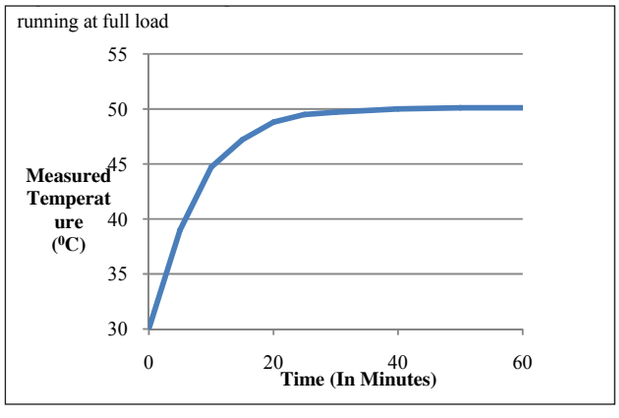

Figure 10: Measured Temperature v/s Time for 2.2kW, 415 V Induction Motor running at full load

6.5 Determination of Rth and Cth for the induction motor

$$\theta(t) = (\theta_{max} - \theta_A)(I/I\_max)^2 \left(1 - e^{-\frac{t}{\tau th}}\right) + \theta_A \tag{55}$$

Thermal Model parameters of induction motor are shown in Table 11 and using equations (56)-(57), Rth and Cth are determined.

Table 11: Thermal Model parameters of induction motor

Parameter	Value
θ_{max}	130 ^{0}C
θ_A	30 ^{0}C
Loading	100%
I	4.5 A

$$Imax = \sqrt{(\theta_{max} - \theta_A)/R.\,Rth} \tag{56}$$
$$\zeta\, th = Rth * \ Cth \tag{57}$$

The temperature rise of the motor under full load conditions is fit using the equation (55) given below,

$$\theta(t) = (\theta_{max} - \theta_A)(I/I\_max)^2 \left(1 - e^{-\frac{t}{\tau th}}\right) + \theta_A$$

The following parameters are determined using the above equations (55)-(57) and shown in Table 12.

Table 12: Thermal Model parameters of induction motor-2

Parameter	Value
I_max	10.03 A
ζ th	7.637 minutes
Rth	0.0989
Cth	77.21

6.6 Effect of Over-voltage

The effect of overvoltage on the loss of life is calculated based on the following parameters shown in Table 13 and the plot is shown in Figure 12.

The test cycle for overvoltage test is explained in the Figure 11. After subjecting the motor to the 100% voltage temperature was measured till 30 minutes until the motor reached a steady state. Then the motor was allowed to cool down for 40 min till the temperature reached to that of the ambient. This was repeated for voltage of 107% and 112%.

Table 13 : Input Data for over-voltage test

Parameter	Value
Ambient Temperature	32.5 ^{0}C
Loading	77 %
Acceleration Factor for Humidity	1
Ea (For Class B Insulation)	0.8 eV [8]
K	0.8614* 10-4 eV/K

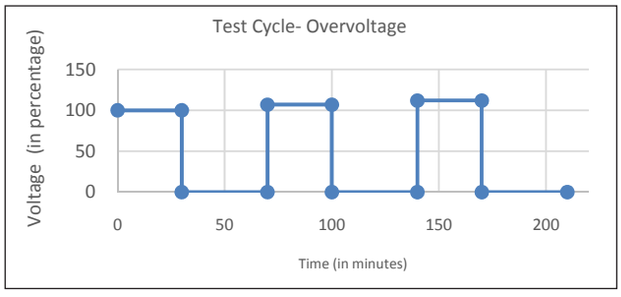

Figure 11: Test cycle for overvoltage test

The following steady state temperatures were observed for the abovementioned conditions as shown in Table 14.

Table 14: Observed temperatures for various voltages

Voltage	Steady State Temperature (^{0}C)
100%	48.5
107%	52.12
112%	54.82

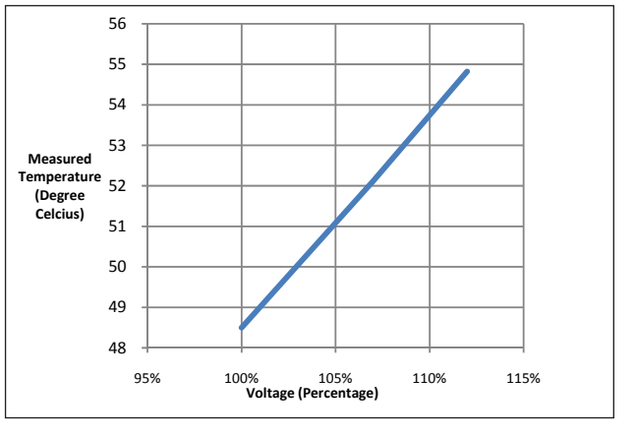

Figure 12: Measured Temperature v/s Voltage (Percentage) for 2.2kW, 415 V Induction Motor running at full load

The following temperatures were input to the ageing model in (58)

$$\ln\left(\frac{tr}{ti}\right) = \left(\frac{Ti}{Tr}\right)\left(\frac{Ea}{k} * \left(\frac{1}{Tr} - \frac{1}{Ti}\right)\right)\left(\frac{Eb}{k} * \left(\frac{1}{RHr} - \frac{1}{RHi}\right)\right) \quad (58)$$

The plot between the Loss of Life and No. of operating hours for various voltages for the motor is given below in figure 13.

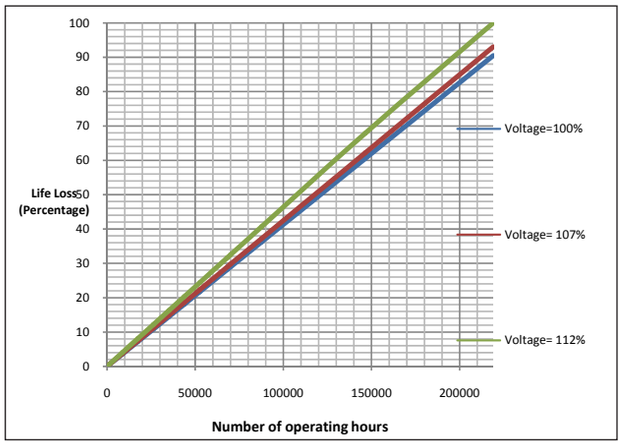

Figure 13: Loss of life v/s No. of operating hours for i) V=100% ii) V=107% ii) V=112%

It is seen that and increased voltage has a detrimental effect on the remaining life. One important factor is the time for which the motor is under the aggravated stress. For shorter durations, it is observed that there is negligible effect on the life loss but as the duration increases, the effect is severe, and i.e. even a 12 % sustained over-voltage can cause an 11% reduction in the life of motor. 100% life loss is obtained at a much shorter duration for V= 112% when the life loss for V= 100% and V= 107% is 90% and 93% respectively. An initial increase of voltage from 100% to 107% causes lesser deterioration than the increase from 107% to 112%. Thus, it can be concluded that rate of ageing or deterioration increases with increase in the value of the applied stress.

6.7 Effect of Unbalance

For the study of unbalance voltages, a rheostat of 12 Ohms, 8.5 A capacity was put in the series of one phase and thus a reduced voltage at one of the phase was observed.

The schematic diagram of the circuit is shown below in Figure 14.

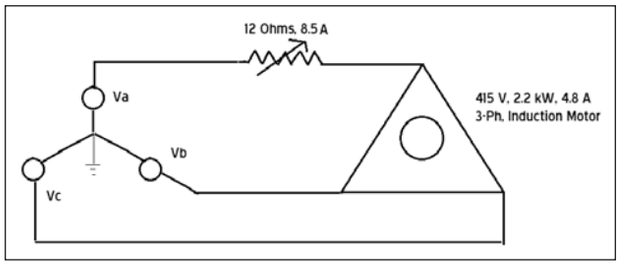

Figure 14: Schematic of voltage-unbalance test

Table 15: Sequence Voltages for different unbalance conditions

Vab (Volts)	Vbc (Volts)	Vca (Volts)	Voltage Unbalance (%)	Positive Sequence Voltage (V1)	Negative Sequence Voltage (V2)
410∠0	410∠0	410∠0	0	410	0
405∠0	411∠-120	410.6∠120	0.6	408.86	-1.83
400.7∠0	412∠-120	412∠120	1.77	408.23	-2.33
395∠0	412∠-120	412∠120	2.78	406.33	-5.66

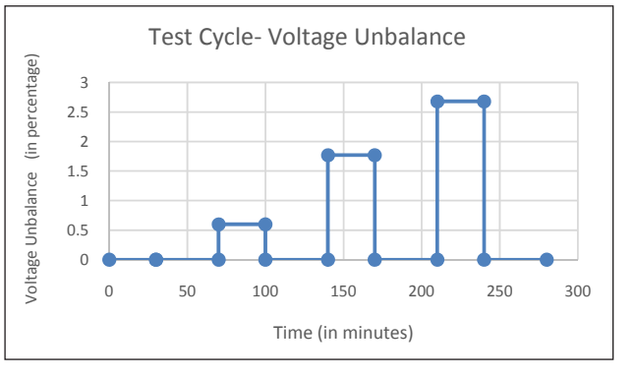

Figure 15: Test cycle for voltage-unbalance test

The test cycle for voltage unbalance test is given in Figure 15. After subjecting the motor to the 0% voltage unbalance, temperature was measured till 30 minutes until the motor reached a steady state temperature value. Then the motor was allowed to cool down for 40 min till the temperature reached to that of the ambient. This was repeated for voltage unbalance of 0.6% , 1.77% and 2.78%.

The positive sequence, negative sequence voltages and voltage unbalance for various cases are tabulated below in Table 15.

The effect of unbalanced voltage on the loss of life is calculated based on the following parameters given in Table 16

Table 16 : Input Data for unbalance test

Parameter	Value
Ambient Temperature	31 ^{0}C
Acceleration Factor for Humidity	1
Ea (For Class B Insulation)	0.8 eV
K	0.8614* 10-4 eV/K

The following steady state temperatures were observed for the abovementioned conditions as given in Table 17.

Table 17: Observed temperatures for various % voltage unbalance

% Unbalance Voltage	Steady State Temperature (^{0}C)
0%	50.1
0.6%	52.12
1.77%	55.82
2.78%	60.62

The plot between Measured Temperature v/s Voltage Unbalance is shown in Figure 16 and is observed that with increase in voltage unbalance the measured temperature increases.

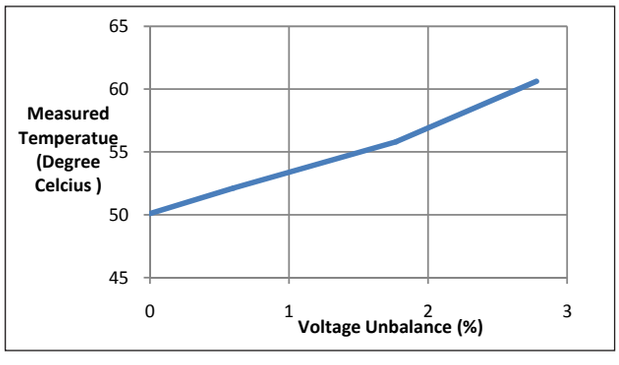

Figure 16: Measured Temperature v/s Voltage Unbalance (Percentage) for 2.2kW, 415 V Induction Motor

The following temperatures were input to the ageing model (Eqn. 58)

$$\ln\left(\frac{tr}{ti}\right) = \left(\frac{Ti}{Tr}\right)\left(\frac{Ea}{k} * \left(\frac{1}{Tr} - \frac{1}{Ti}\right)\right)\left(\frac{Eb}{k} * \left(\frac{1}{RHr} - \frac{1}{RHi}\right)\right)$$

From the plot between Loss of life v/s No. of operating hours for Voltage Unbalance in Figure 17, it is seen that when the Voltage unbalance is more, the loss of life is faster.

It is seen that and unbalanced voltages also has a negative effect on the remaining life. In this study, unbalance in one of the phases of the 3 phase induction motor was created by adding a resistor in series with the phase winding. By changing the value of the

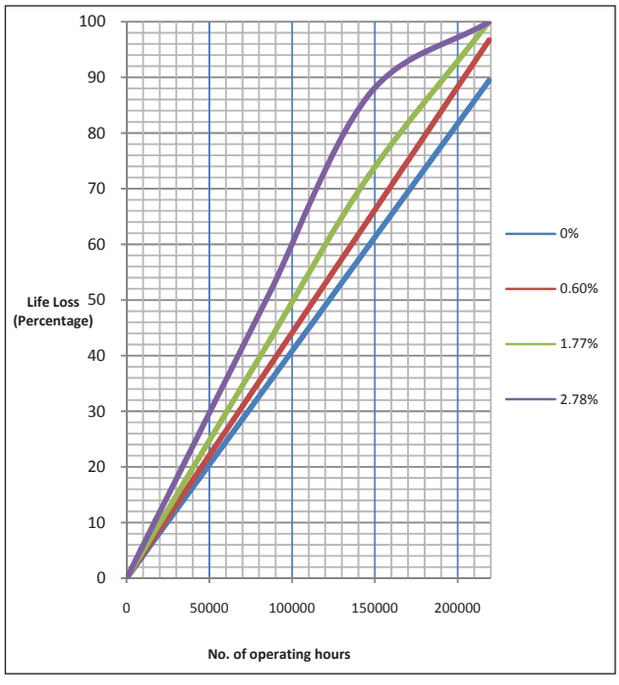

Figure 17: Loss of life v/s No. of operating hours for Voltage Unbalance i) 0% ii) 0.6% iii) 1.77% iv) 2.78 %

resistor, reduced voltage was developed in one of the phases and thus unbalance of 0.6%, 1.77% and 2.78% were derived using the resistor. Then for all these cases, the stator winding temperature was found and the curves for life loss with no. of operating hours were drawn. It was observed that, one important factor in the estimation of life loss due to unbalance is the time for which the motor is under the aggravated stress. For shorter durations, it is observed that there is negligible effect on the life loss but as the duration increases, the effect is severe, and i.e. even a 2.78 % sustained unbalance can cause a 12 % reduction in the life of motor. 100% life loss is obtained at a much shorter duration for Unbalance= 2.78% when the life loss for Unbalance= 0% and Unbalance=0.6 % is 89% and 96% respectively. An initial increase of unbalance from 0% to 0.6% causes lesser deterioration than the increase from 0.6% to 1.77% and from 1.77% to 2.78%. Thus, it can be concluded that rate of ageing or deterioration increases with increase in the value of the applied stress.

7. Conclusion

Winding failure accounts for a major portion of induction motor failures. Thus it becomes pivotal that the concept of winding failure is understood fully and efforts shall be made to minimize any mal-operation due to winding failure. This work has attempted to analyse the induction motor winding failure through the lens of an integrated approach which combines the electrical, thermal and ageing aspect of a motor winding and hence predict its remaining life/loss of life. This is a new domain as the it involves an amalgamation of the electrical, thermal and ageing aspect of a motor to determine its life.

The integrated model comprising the electrical, thermal and ageing model as discussed above was used to quantify the loss of life of a 2.3 kW, 415 V induction motor under different operating anomalies e.g. overvoltage, unbalance, etc. In the present work, the induction motor circuit derived using No load and Blocked Rotor test gives the winding losses which goes as an input to the thermal model to give the winding temperature. This winding temperature goes as an input to the ageing model, which basically uses temperature and humidity as the stresses (Eyring Model) to estimate the remaining life. The effect of various starts/stops on the remaining life is also seen.

References

1. M. Vfflaran and M. Subudhi "Aging Assessment of Large Electric Motors in Nuclear Power Plants", Brookhaven National Laboratory, March 1996.
2. E.Anbarasu and M.Karthikeyan "Modeling of Induction Motor and Fault Analysis", International Journal of Engineering Science and Innovation Technology (IJESIT), Volume 2, Issue 4, July 2013.
3. NEMA MG-1-25 Motors and Generators –Classification of Insulation System.
4. Mahfoud Chafai, Larbi Refoufi , Hamid Bentarzi "Reliability Assessment and Improvement of Large Power Induction Motor Winding Insulation Protection System Using Predictive Analysis" ,WSEAS Transactions On Circuits And Systems, Issue 4, Volume 7, April 2008.
5. J.B. Gupta, Electrical Machines-Induction Motor- No-Load Test and Blocked Rotor Test , Page 399- 406 ,Edition 2007
6. Arafat Siddique, G.S.Yadava and Bhim Singh "Effects of Voltage Unbalance on Induction Motors", Conference Record of the 2004 IEEE International Symposium on Elecnical Insulation, Indianapolis, IN USA, 19-22 September 2004.
7. Zhi Gao "Sensorless Stator Winding Temperature Estimation for Induction Machines" ,Georgia Institute of Technology, December 2006.
8. Emanuel L. Brancato "Estimation of Lifetime Expectancies of Motors", IEEE Electrical Insulation Magazine May/June 1992.
9. Pragasen Pillay and Marubini Manyage "Loss of Life in Induction Machines Operating with Unbalanced Supplies", IEEE Transactions On Energy Conversion, VOL. 21, NO. 4, December 2006.
10. Jose Policarpo G. de Abreu and Alexander Eigeles Emanuel," Induction Motor Thermal Aging Caused by Voltage Distortion and Imbalance: Loss of Useful Life and Its Estimated Cost", IEEE Transactions On Industry Applications, Vol. 38, No. 1, January/February 2002.

Life Cycle Reliability and Safety Engineering
Vol.5 Issue 1 (2016) 43-50

Life Estimation of I&C Cable Insulation Materials based on Accelerated Life Testing

T. V. Santhosh, P. K. Ramteke, N. B. Shrestha, A. K. Ahirwar and V. Gopika
Reactor Safety Division, Bhabha Atomic Research Centre, Trombay, Mumbai, India.
Email: santutv@barc.gov.in

Abstract

Accelerated life tests are becoming increasingly popular in today's industry due to the need for obtaining life data quickly and reliably. Life testing of products under higher stress levels without introducing additional failure modes can provide significant savings of both time and money. Correct analysis of data gathered via such accelerated life testing will yield parameters and other information for the product's life under use stress conditions. To be of practical use in assessing the operational behaviour of cables in NPPs, laboratory ageing aims to mimic the type of degradation observed under operational conditions. Conditions of testing therefore need to be carefully chosen to ensure that the degradation mechanisms occurring in the accelerated tests are similar to those which occur in service. This paper presents the results of an investigation in which the elongation-at-break (EAB) measurements were carried out on a typical control cable to predict the mean life at service conditions. A low voltage polyvinyl chloride (PVC) insulated and PVC sheathed control cable, used in NPP instrumentation and control (I&C) applications, was subjected to thermal ageing at three elevated temperatures. Tensile testing was performed using Tinius Olsen Universal Testing Machine with a load cell of 10kN to determine elongation at break (EAB). A minimum of 7 samples were tested under each ageing condition to build the confidence in the results. Analysis of variance (Anova) was also performed at specific ageing conditions to study the degree of degradation due to thermal ageing. Since Anova assumes that the data is normally distributed, an Anderson-Darling normality test was also performed at each ageing condition. The data was analyzed to find the best fit model to determine the ageing time corresponding to 50% EAB. From the experimental evaluations and using Arrhenius theory, the mean life corresponding to service condition is found to be 6.75 years for the sheath and 21.1 years for the insulation. It should be noted here that the mean life estimated is completely based on the mechanical properties of the material subjected to accelerated ageing conditions.

Keywords: *Accelerated life testing, instrumentation and control cables, condition monitoring, elongation-at-break, tensile testing, analysis of variance, and nuclear power plants.*

1. Introduction

Instrumentation and control (I&C) cables operating in NPP service are exposed to a variety of environmental and operational stressors. Over time, these stressors, and combinations of these stressors, can cause ageing and degradation mechanisms that will result in a gradual degradation of the cable insulation and jacket materials. Much of the degradation due to ageing is controlled through periodic maintenance and/or component replacement. However, I&C cables do not receive periodic maintenance or monitoring once they are installed. Moreover, replacing a cable in an NPP can be a complex and expensive task. Most of the work on degradation of cable insulation and life assessment discusses about the traditional methods of monitoring the cable degradation through parameters such as elongation at break (EAB), insulation resistance (IR), oxidation induction time (OIT), etc. In general, many plants perform IR testing or measure polarization index (PI), and some plants additionally perform time domain reflectometry (TDR), Fourier transform infrared (FTIR) spectroscopy, etc[1-3]. However, attempts at gleaning any useful information on the remaining life from such measurements also raise few questions. The best conclusion that can be drawn from such testing is the electric insulation is acceptable at present with no guarantee for future continued integrity of operational acceptability [4].

The state-of-the-art for incorporating cable ageing effects into probabilistic safety assessment (PSA) is still

evolving and current assumptions that need to be made on the failure rate and common cause effects are based on limited data. In the assessment of reliability of NPP systems, the ageing effect of electrical cable insulation is generally not considered and also, there is no standard methodology or framework that exists for incorporating such ageing effects into the system reliability. Therefore, identification and quantification of ageing of electrical cables is very much essential for an accurate prediction of system reliability for PSA applications.

This study aims to develop the background and technical basis for incorporating the ageing effects of I&C cables in the assessment of reliability of safety related systems in nuclear power plants.The polyvinylchloride (PVC) based I&C cable insulation materials were subjected to accelerated thermal ageing and the properties such as elongation-at-break, tensile strength, etc. were measured to develop remaining life prediction models. Analysis of variance (Anova) was performed at specific ageing conditions to study the degree of degradation due to thermal ageing. Since Anova assumes that the data is normally distributed, an Anderson-Darling normality test was also performed at each ageing condition. The data was analyzed to find the best fit model to determine the ageing time corresponding to 50% EAB. From the experimental evaluations and using Arrhenius theory, the mean life corresponding to service condition was predicted for both insulation and sheath.

2. Accelerated Life Testing

The accelerated thermal ageing is a means of obtaining the failure characteristic of an item/ equipment by subjecting to higher stress conditions. The results of accelerated tests will be correlated against the field ageing conditions in order to determine the remaining useful life. These tests are performed at relatively higher stress conditions compared to the normal use conditions to observe the failures in very short time duration. Accelerated life tests are becoming increasingly popular in today's industry due to the need for obtaining life data quickly and reliably. Life testing of products under higher stress levels without introducing additional failure modes can provide significant savings of both time and money. Correct analysis of data gathered via such accelerated life testing will yield parameters and other information for the product's life under use stress conditions. To be of practical use in assessing the operational behaviour of cables in NPPs, laboratory ageing aims to mimic the type of degradation observed under operational conditions. Conditions of testing therefore need to be carefully chosen to ensure that the degradation mechanisms occurring in the accelerated tests are similar to those which occur in service. Accelerated life testing involves acceleration of failures with the single purpose of the "quantification of the life characteristics of the product at normal use conditions"[5]. Generally, accelerated tests can be divided into three types:

2.1 Qualitative Tests

Qualitative tests are performed on small samples with the specimens subjected to a single severe level of stress, to a number of stresses, or to a time-varying stress (i.e., stress cycling, cold to hot, etc.). If the specimen survives, it passes the test. Otherwise, appropriate actions will be taken to improve the product's design in order to eliminate the cause(s) of failure. Qualitative tests are used primarily to reveal probable failure modes. However, if not designed properly, they may cause the product to fail due to modes that would have never been encountered in real life.Qualitative tests are tests that yield failure information (or failure modes) only. They have been referred to by many names including: (i) Elephant Tests, (ii) Torture Tests, (iii) HALT(Highly Accelerated Life Testing), and (iv) Shake & Bake Tests.

2.2 Environmental Stress Screening and Burn-in

The second type of accelerated test consists of environmental stress screening (ESS) and Burn-in testing. ESS is a process involving the application of environmental stimuli to products (usually electronic or electromechanical products) on an accelerated basis. The stimuli in an ESS test can include thermal cycling, random vibration, electrical stresses, etc. The goal of ESS is to expose, identify and eliminate latent defects which cannot be detected by visual inspection or electrical testing but which will cause failures in the field. ESS is performed on the entire population and does not involve sampling.Burn-in can be regarded as a special case of ESS. According to MIL-STD-883C, Burn-in is a test performed for the purpose of screening or eliminating marginal devices. Marginal devices are those with inherent defects or defects resulting from manufacturing aberrations which cause time and stress-dependent failures. As with ESS, Burn-in is performed on the entire population.

2.3 Quantitative Accelerated Life Tests

Quantitative accelerated life testing consists of

tests designed to quantify the life characteristics of the product, component or system under normal use conditions, and thereby provide reliability information. Reliability information can include the determination of the probability of failure of the product under use conditions, mean life under use conditions, and projected returns and warranty costs. It can also be used to assist in the performance of risk assessments, design comparisons, etc. Accelerated life testing can take the form of usage rate acceleration or overstress acceleration.

3. Thermal Ageing

Polymeric cable materials used in NPP have a finite life in an environment featuring elevated temperatures and radiation. Recognizing this fact, industry standards and the National Regulatory Commission (NRC) have obligated nuclear utilities to provide evidence showing that degradation caused by ageing will not critically affect the performance of these materials and will not pose any safety hazards during their qualified service life of 40 years. Because it is impractical to test these materials under normal plant conditions (natural aging), accelerated aging is usually employed for qualification [6].

3.1 Arrhenius Theory

In 1884,a Swedish chemist named Arrhenius developedan equation to correlate the rate of a chemical reaction with the absolute temperature of the reacting materials,and a constant for that reaction called its "Activation Energy". This constant may be visualized as an energybarrier which must be overcome before the reaction canproceed. The number of molecules active enough toovercome this barrier increases with temperature; at lowtemperatures, the number may be so few that for allpractical purposes the reaction is not noticeable. Prediction of aging performance using accelerated aging tests based on Arrhenius theory has been practiced for years. However, it is a practice that has attracted considerable controversy due to the limitations of this theory and the scarcity of empirical verification. To allow for uncertainties, conditions for accelerated aging tests are often made purposefully conservative[7]. Experience has suggested that they may be unrealistically conservative, leading to frequent and expensive replacements, and the use of materials which may not be otherwise optimal.

According to standards [8-10], the simulation of long-term service thermal ageing is performed isothermally at elevated temperature using Arrhenius methodology. The Arrhenius model, describes the relationship between rate of degradation, the ageing temperature and the duration of exposure. The model estimates the time to reach the end point of the material's life by the following equation.

$$t = Ae^{\frac{\Phi}{kT}} \quad (1)$$

Where, t represents a quantifiable life measure, such as mean life, characteristic life, median life, etc., T represents the stress level (in absolute units if it is temperature), A is a model parameter to be determined, Φ is activation energy in eV, and k is the Boltzmann constant (8.617e-5eV/K).

Most practitioners use the term acceleration factor to refer to the ratio of the life between the use level and a higher test stress level.

$$A_F = \frac{t_{use}}{t_{accelerated}} \quad (2)$$

For reliable simulation of long-term thermal ageing, the temperature of accelerated ageing should not be too far from the service temperature. The standards recommend using not more the 25^0C difference. But to simulate 40 years of service ageing, such a small difference would lead to very long testing time. Hence, the test temperature is usually higher. The maximum allowed ageing temperature is limited by the range of chemical stability (the temperature range in which for specific time no chemical changes are detected) or by any thermo-dynamical transition in the material, like glass transition (Tg), softening or melting point.

4. Experimental

Experimental techniques can provide the means for evaluating the level of ageing and degradation of electrical cable insulation materials. Condition monitoring for electric cable systems involves inspection and measurement of one or more indicators, which can be correlated to the condition or functional performance of the electrical cable on which it is applied [11-14]. Furthermore, it is desirable to link the measured indicators such as elongation at break (EAB), insulation resistance (IR), etc. with an independent parameter, such as time or cycles, in order to identify trends in the condition of the cable [15-16].

4.1 Accelerated Thermal Ageing

The cables chosen for experiments are of low voltage type (≤ 1100V) as they are extensively being used in nuclear power plant I&C applications. The specifications of the cable chosen for thermal ageing experiments are shown in Table 1.

Table 1: Specifications Of Cable For Thermal Ageing

Cable type	Specifications	Polymer type	
		Insulation	Sheath
Control cable	19 core, 1.5sq. mm, 650/1100V	PVC	PVC

The samples of sheath material were made according to ASME D638-10 standard and the

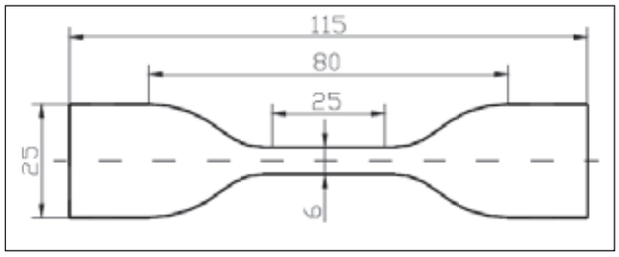

Fig.1: Specimen of Sheath (dumbbell shaped)

specimen sample of sheath is shown in Figure 1. However, in case of insulation, the tubular samples of length 10cm were used due to their small cross-sectional area.

The test temperatures were selected based on the guidelines suggested in IEC 60216 [27] and the test matrix adopted for both insulation and sheath isshown in Table 2.

Table 2: Samples

Ageing time (Days)	Test Temperature (^{0}C)		
	90	100	110
	Number of samples under test		
0	7		
5	7	7	7
10	7	7	7
15	7	7	7
20	7	7	7

Accelerated thermal ageing test was carried out in oven with forced air circulation with accuracy of ±1^{0}C. During the accelerated thermal ageing test, test parameters monitored were the visual inspection and cracks on bending. The samples were taken out according to the test matrix for EAB measurement.

B. Elongation-at-break Measurement

Elongation-at-break (EAB) is a measure of a material's resistance to fracture under an applied tensile stress and is often termed the ductility of a material. When exposed to stressors such as elevated temperature and radiation levels, polymers tend to lose their ductility. The rate of ductility loss is determined by the material composition, as well as the severity of the stressors; however, in general, ductility will decrease with age. EAB has been shown to be a very accurate and repeatable method of monitoring polymer condition.Tensile tests were performed using Tinius Olsen Universal Testing Machine with a load cell of 10kN in accordance with ASTM Standard D638, D412 and IS 10810 Part 7. Tests were performed with an initial jaw separation of 25mm at a strain rate of 15 mm/min. with the extensometer the mechanical properties such as tensile strength, elongation at break, etc. were recorded.

5. Results and Discussion

The results of tensile testing after thermal ageing are shown here in the form of Stress-Strain curves and EAB as a function of ageing time for various temperatures.

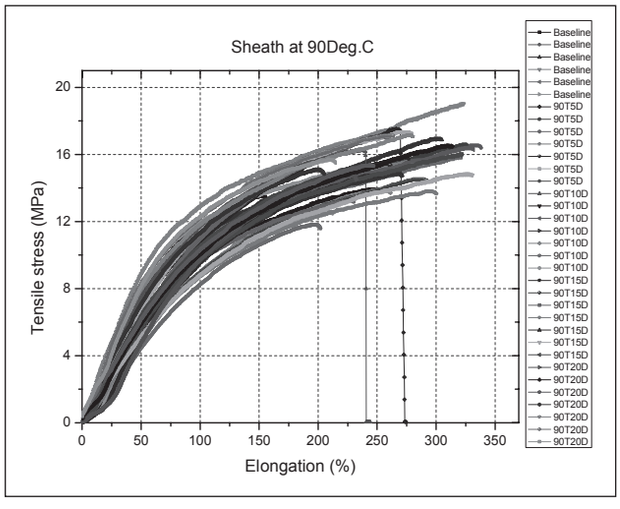

Fig.2: Stress-strain curves for sheath at 90˚C

5.1 Stress-Strain Curves

The curves shown in Figures 2-7 indicate the change in mechanical properties as a function of time and temperature.

The baseline refers to unaged/fresh samples, whereas example, 90T10D refers to samples aged for 10 days at 90˚C.

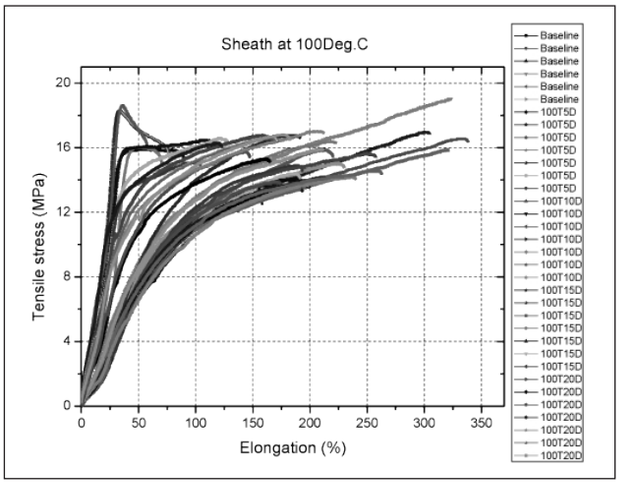

Fig.3: Stress-strain curves for sheath at 100˚C

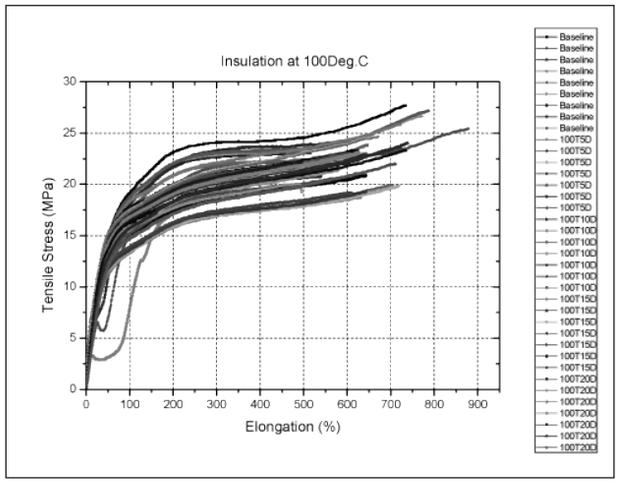

Fig.6: Stress-strain curves for insulation at 100˚C

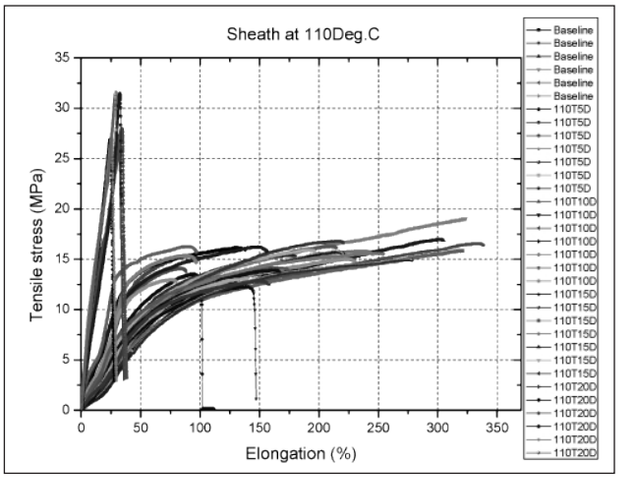

Fig.4: Stress-strain curves for sheath at 110˚C

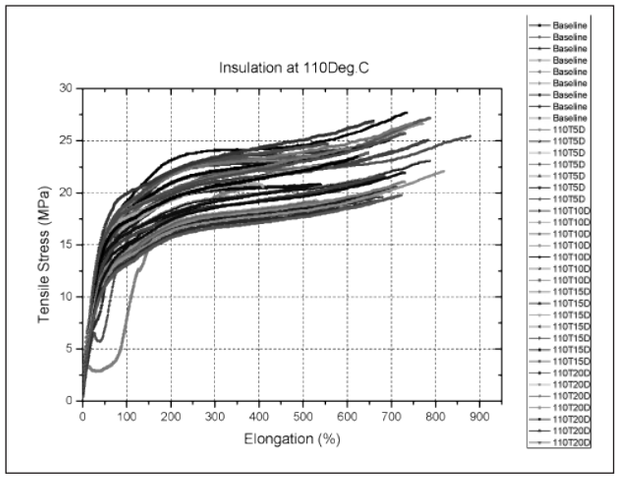

Fig.7: Stress-strain curves for insulation at 110˚C

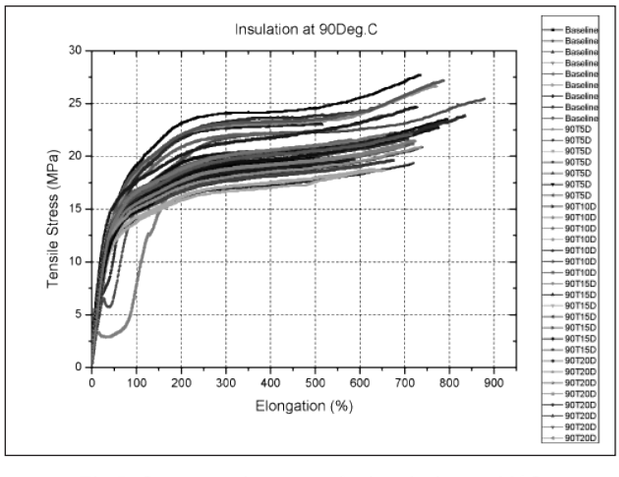

Fig.5: Stress-strain curves for insulation at 90˚C

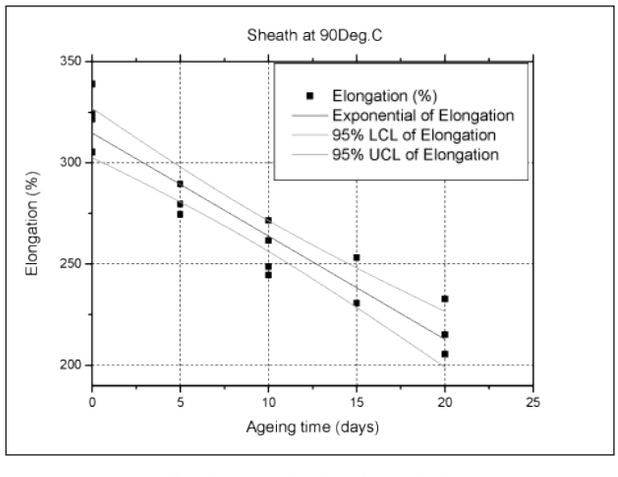

Fig.8: EAB for sheath at 90˚C

5.2 Elongation-at-break

The data obtained from tensile testing was analyzed through regression analysis to assess the ageing effect on elongation. EAB as a function of ageing time for insulation and sheath are shown in Figures 8-13.

6. Mean Life Estimation

In typical life data analysis one determines, through

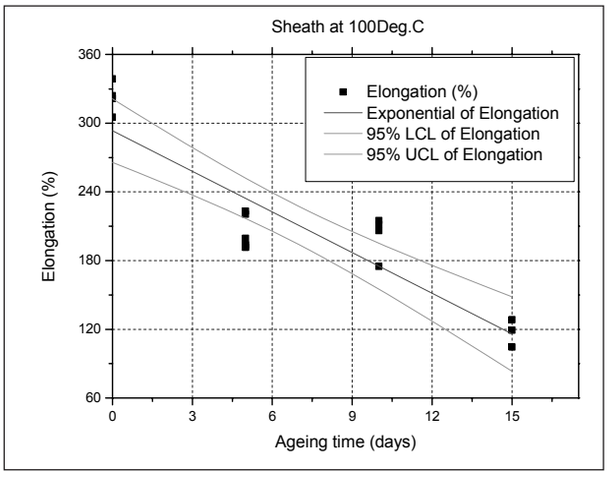

Fig.10: EAB for sheath at 110˚C

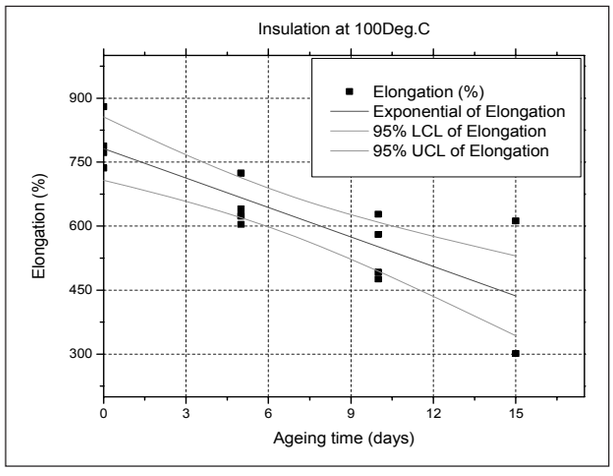

Fig.12: EAB for insulation at 100˚C

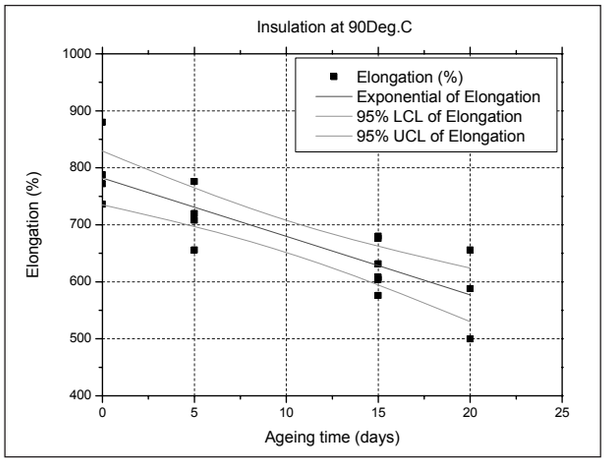

Figure 11: EAB for insulation at 90˚C

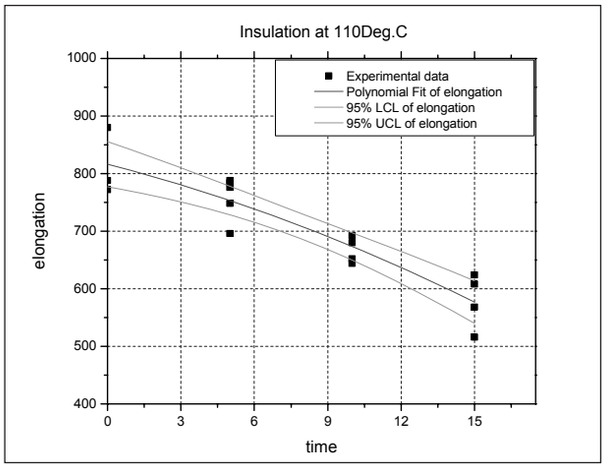

Fig.13: EAB for insulation at 110˚C

Table 3: TTF For Sheath

Temperature (˚C)	Regression model	Equation	TTF (days)
90	Exponential	$\mathrm{EAB} = 63270 - 62955\exp\big((8.08\mathrm{E}-5)*\mathrm{t}\big)$	52
100	Exponential	$\mathrm{EAB} = 139242 - 138948\exp((8.5\mathrm{E}-5)*\mathrm{t})$	21
110	Polynomial	$EAB = 328 - 30.5 * t + 0.79 * t^2$	15

Table 4: TTF For Insulation

Temperature (˚C)	Regression model	Equation	TTF (days)
90	Exponential	$\mathrm{EAB} = 54606 - 53823\exp((1.9\mathrm{E}-4)*\mathrm{t})$	71
100	Exponential	$\mathrm{EAB} = 184937 - 184155\exp((1.25\mathrm{E}-4)*\mathrm{t})$	32
110	Exponential	$\mathrm{EAB} = 1109.84 - 292.75\exp((3.9\mathrm{E}-2)*\mathrm{t}$	65

the use of statistical distributions, a life distribution that describes the times-to-failure of a product. Statistically speaking, one wishes to determine the use level probability density function (PDF) of the times-to-failure. In typical life data analysis, this use level PDF of the times-to-failure can be easily determined using regular times-to-failure data and an underlying distribution such as the Weibull, exponential, and lognormal distributions. Generally, in life estimation studies under accelerated ageing conditions, a Weibull distribution is considered to be an appropriate failure distribution when the failure data is very limited.

A. Estimation of ageing time corresponding to 50% absolute EAB

In order for the life prediction, the times-to-failure (TTF) corresponding to the desired failure criterion (50% absolute EAB) needs to be estimated from the experimentally derived empirical models. The estimated TTFs for sheath and insulation are shown in Table III and IV respectively.

6.2 Life Estimation for Sheath

The Arrhenius plot of the TTF data of sheath is shown in Figure 14.

The parameter values of the Arrhenius plot with coefficient of determination being 0.88 are shown in Table V and the corresponding linear model is shown in Equation (3).

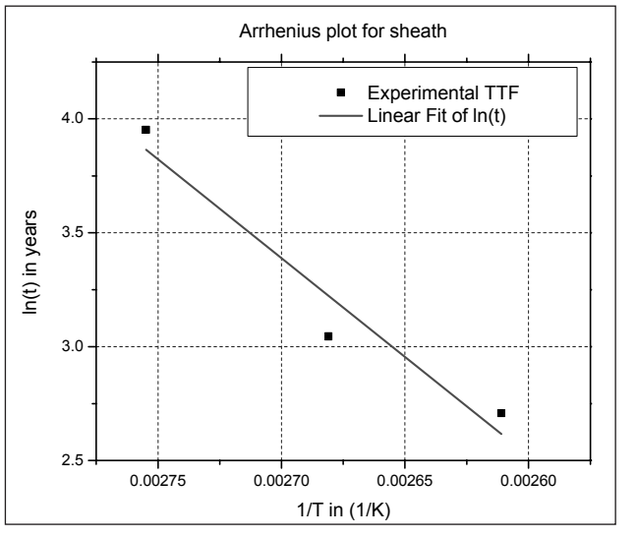

Figure 14: Arrhenius plot for sheath

Table 5: Parameters of Arrhenius Plot

Parameter	Value	Standard error
a	-20.03	5.78
b	8675.34	2154.36

$$\ln(t) = \mathrm{a} + b\frac{1}{T} \quad (3)$$

Here, $b = slope = \frac{\Phi}{k}$, hence, activation energy is found to be 0.765eV. From the Arrhenius, the model constant, A, in Equation (1) is found to be 1.9905E-09. Substituting these values in Arrhenius equation, the mean life for sheath corresponding to service condition (40°C) is found to be 6.75 years.

6.3 Life Estimation for Insulation

It can be seen from Table IV that Arrhenius plot cannot be constructed for the insulation due to limited data points. Hence, it is recommended to use the analytical formulation and predict the life by Arrhenius equation as shown in Equation (1). From the Arrhenius factor approach as shown in Equation (4), and considering first two temperatures, the activation energy is found to be 0.9279eV and the model constant, A, from Equation (1) at one of the test temperature is found to be 1.0288e-11.using these predicted values of activation energy and model constant, the mean life of the insulation under use conditions (40^0C) is found to be 21.1 years for the insulation.

$$\ln\left(\frac{t1}{t2}\right) = \left(\frac{\Phi}{k}\right)\left(\frac{1}{T1} - \frac{1}{T2}\right) \quad (4)$$

7. Reliability Prediction

In order for the reliability prediction, an appropriate life distribution is chosen to describe the failure characteristics. The Weibull distribution is commonly used in reliability studies and it is well suited to fitting the 'weakest-link' properties of typical lifetime data. Different mechanisms of failure can sometimes be distinguished by the Weibull parameters needed to fit the results. The reliability function from Weibull distribution is given by:

$$\boldsymbol{R(t) = e^{-\left(\frac{t}{\eta}\right)^{\beta}}} \quad (5)$$

Where, η is the scale parameter or characteristic life, β is the shape parameter and t is the time. Since mean life predicted from Arrhenius approach is equivalent to characteristic life, the parameter, η in Equation (5) can be replaced by the predicted mean life. Hence,the time dependent reliability can be determined for different values of β to account for various failure characteristics. Now with η=6.75years

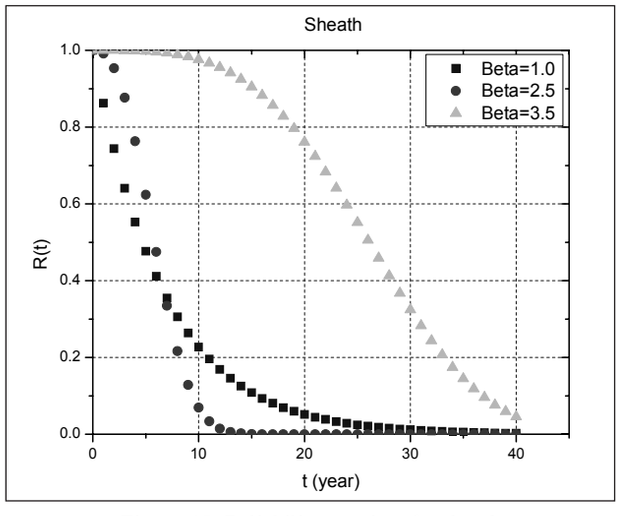

Figure 15: Reliability vs. time for sheath

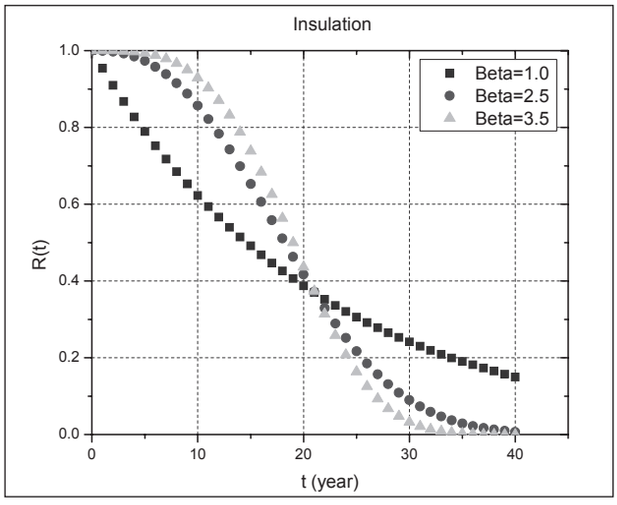

Figure 16: Reliability vs. time for insulation

for sheath and 21.1 years for insulation, and varying t from 0 to 40years, the time dependent reliabilities of the thermally aged cable sheath and insulation are shown in Figure 15 and 16 respectivelyfor different values of β.

8. Conclusions

The thermal ageing of sheath and insulation of I&C cable has been carried out in order to determine their mean life. From the experimental evaluations, considering use conditions (40^0C) for I&C cable predicted mean life is found to be 6.75 years for the sheath and 21.1 years for the insulation. From the Weibull reliability theory, the time dependent reliabilities under useful conditions have also been predicted for both sheath and insulation materials. the predicted reliabilities can be useful for incorporating the cable ageing into PSA of NPPs. However, it should be noted here that the mean life estimated are merelybased on the mechanical properties of the material subjected to accelerated ageing conditions. Neither the generic data nor the failure history of the sheath and insulation has been considered in this study.

References

1. S.G. Burnay, An overview of polymer ageing studies in the nuclear power industry, Nuclear Instruments and Methods in Physics Research B, Vol. 185, pp. 4-7, 2001.
2. R. Clavreul, Ageing of polymers in electrical equipment used in nuclear power plants, Nuclear Instruments and Methods in Physics Research B, vol. 151, pp. 449-452, 1999.
3. G.E. Sliter, Overview of research on nuclear plant cable ageing and life extension, in Proc. SMiRT-12, Elsevier Science Publishers, pp. 199-203, 1993.
4. D.A. Horvath, D.C Wood and M.J. Wylie, Microscopic void characterization for assessing ageing of electrical cable insulation used in nuclear power stations, in Proc. IEEE conference on electrical insulation and dielectric phenomena (CEIDP 2000), Victoria, BC, pp. 1-5, October, 2000.
5. Luis A. Escobar and William Q. Meeker, A Review of Accelerated Test Models, Statistical Science, vol. 21, no. 4, pp. 552–577, 2006.
6. Nicola Bowler and Shuaishuai Liu, Aging Mechanisms and Monitoring of Cable Polymers, International Journal of Prognostics and Health Management, ISSN 2153-2648, no. 029, 2015.
7. A. S. Maxwell, W. R. Broughton, G. Dean and G. D. Sims, Review of accelerated ageing methods and lifetime prediction techniques for polymeric materials, National Physical Laboratory, 2005.
8. IEC 216, Guide for the determination of thermal endurance properties of electrical insulating materials, 4th issue (1990-1994).
9. IEEE Std. 323-1974: IEEE Standard for Qualifying Class 1E Equipment for Nuclear Power Generating Stations, Institute of electrical and electronics engineers, New York, 1974.
10. IEEE Std. 383-1974, "IEEE standard for type test of class 1E electrical cables, field splices, and connections for nuclear power generating stations", Institute of electrical and electronics engineers, New York, 1974.
11. IAEA-TECDOC-932, Pilot study on the management of ageing of instrumentation and control cables, International Atomic Energy Agency, 1997.
12. K. Anandakumaran, W. Seidl, P.V. Castaldo, Condition assessment of cable insulation systems in operating nuclear power plants, IEEE transactions on dielectrics and electrical insulation, vol. 6, no. 3, pp. 376-384, 1999.
13. IAEA-TECDOC-1188, Assessment and management of ageing of major nuclear power plant components important to safety: In-containment instrumentation and control cables, vol. I, International Atomic Energy Agency, 2000.
14. IAEA-TECDOC-1188, Assessment and management of ageing of major nuclear power plant components important to safety: In-containment instrumentation and control cables, vol. II, International Atomic Energy Agency, December 2000.
15. K. T. Gillen, M. Celina, R. L. Clough and J. Wise, Extrapolation of accelerated aging data- Arrhenius or Erroneous?, Review paper in Trends in Polymer Science, no. 5, pp. 250, 1997.
16. G. Mazzanti, G.C. Montanari and A. Motori, An insight into thermal life testing and characterization of EPR insulated cables, Journal of physics D: Applied physics, No. 27, pp. 2601-2611, 1994.
17. ASTM D638, Standard Test Method for Tensile Properties of Plastics, ASTM International, 2002.
18. IS 10810 (Part 43)-1984, Methods of test for cables: Insulation resistance, 1984

SRESA JOURNAL SUBSCRIPTION FORM

Subscriber Information (Individual)

Title	First Name	Middle Name	Last Name
_____	_____	_____	_____

Street Address Line 1	Street Address line 2
_____	_____

City	State/Province	Postal Code	Country
_____	_____	_____	_____

Work Phone	Home Phone	E-mail address
_____	_____	_____

Subscriber Information (Institution)

Name of Institution/ Library _____

Name and Designation of Authority for Correspondence _____

Address of the Institution/Library _____

Subscription Rates

	Subscription Quantity	Rate	Total
Annual Subscription (in India)	_____	Rs. 15, 000	_____
(Abroad)	_____	$ 500	_____
	_____		_____
	_____		_____

Payment mode (please mark)

Cheque ☐ Credit Card ☐ Master Card ☐ Visa ☐ Online Banking ☐ Cash ☐ De mand Draft ☐

Credit card Number _____

Credit Card Holders Name _____

Credit Card Holde _____